The structure and evolution of flow fields and other vector fields

1978 J. Phys. A: Math. Gen. 11 1455

(http://iopscience.iop.org/0305-4470/11/8/009)

J. Phys. A: Math. Gen. Vol. 11, No. 8, 1978. Printed in Great Britain

The structure and evolution of flow fields and other vector fields

A S Thorndike†, C R Cooley† and J F Nye‡

† Arctic Ice Dynamics Joint Experiment, Division of Marine Resources, University of Washington, USA

‡ H H Wills Physics Laboratory, University of Bristol, England

Received 17 October 1977, in final form 17 March 1978

Abstract. General two-dimensional flow fields, or other vector fields, contain singularities. The singularities can be classified (Whitney 1955) as either folds, which are lines, or as cusps, which are isolated points on the fold lines. As the field evolves with time, discrete events occur which alter the patterns of folds and cusps. Thom's (1975) list of elementary catastrophes describes these events when the changes in the field are the result of changes of an underlying scalar generating function. In that case the generic events are lips, beak-to-beak, swallowtail, hyperbolic umbilic and elliptic umbilic. If the vector field evolves with time in a more general way, the only generic events are lips, beak-to-beak, and swallowtail.

Similarly, in a three-dimensional vector field constrained by being derived from an underlying generating function, the generic singularities are the first five in Thom's list: the fold, cusp, swallowtail, elliptic and hyperbolic umbilic; but when the field is not constrained in this way, only the fold, cusp and swallowtail will occur generically.

Two geophysical illustrations are used. In the first the geostrophic wind is derived from measured values of surface pressure. The surface pressure field is used to construct a generating function, and Thom's list applies under the hypothesis that changes of the wind arise only from changes of the pressure field. The roles of umbilic points and 'antiumbilic lines' in the pressure field are discussed. In the second illustration measured values of the velocity field of drifting sea ice are used. Here the shorter list of events applies because the velocity field itself is subject to change. Since the velocity field is not generated from a surface (provided in the first illustration by the pressure field) there are no longer any umbilic points, but the concept is readily generalised. There are six kinds of generalised umbilic (isotropic) points and they occur in the two-dimensional field of any symmetric tensor. They correspond to the four kinds of umbilic points of a surface classified by Berry and Hannay (1977). In similar way there are six kinds of generalised antiumbilic points.

The significance of the work is that the singularities represent topological structure in a vector field; they characterise its anatomy and thus enable one to give an answer to the question, 'when are two fields similar?' Within the class of fields studied the work identifies those features that will occur naturally, as distinct from special features that can result only from added physical constraints.

1. Introduction

In this paper we describe a way of characterising the basic structure of a flow field. This is achieved by studying a certain class of singularities in the field. The singularities we treat are generic: that is to say, they will occur naturally in a general field. They are invariant under small perturbations to the field, and they have a basic geometric significance. Most of the discussion emphasises two-dimensional flow fields

0305-4770/78/0008-1455$03.00

and their evolution in time, but the results are also applied to three-dimensional flow fields. Possible applications to other three-dimensional vector fields—electric or magnetic fields, say—are immediate.

Section 2 describes a mapping, which is central to our treatment, from the two-dimensional space of the flow field to two-dimensional velocity space, and draws on the classic result of Whitney (1955) that generically only two kinds of singularities in this mapping are possible—the fold and the cusp. To help relate these ideas to more familiar kinematic quantities such as divergence, shear and vorticity we describe their meaning for the particular cases of irrotational and incompressible flow.

For time-dependent flow fields (§ 3) the folds and cusps in the velocity mapping will move continuously, but their general pattern will not change except at isolated points in space and time; we call such points *events*. The singularities are stable features of the flow, in the sense that they persist under small perturbations of the flow. Section 3 discusses this concept and also establishes the connection with catastrophe theory. The closest previous work we know of that connects flow fields with catastrophe theory is that of Berry and Mackley (1977), but our point of view is different from theirs. (See also Lacher *et al* 1977 and Benjamin 1978.) We relate the two approaches in appendix 1.

The problem is now to identify the possible events. When the flow is subject only to perturbations of an underlying generating function, Thom's list of elementary catastrophes of co-dimension 3 is used to provide the answer. Examples are given (§ 4) from the geostrophic flow of the atmosphere, where the atmospheric surface pressure field ensures an underlying generating function. Special points, *umbilic* points, exist in the flow where the two principal curvatures of the pressure surface are equal. Umbilic points in surfaces have been classified by Berry and Hannay (1977). They are important here (together with another class of points where the principal curvatures are equal and opposite, which we call *antiumbilic* points) because they are special points in a pattern of lines which helps to locate cusp points, and because they participate intimately in two of the events we describe. Up to this point in the paper the results, if not the point of view, are in complete analogy with applications of catastrophe theory to problems in geometrical optics (Berry 1976, Berry and Nye 1977, Nye 1978).

In § 5 stability is defined with respect to perturbations of the flow field itself, rather than of an underlying generating function. Since this is a larger class of perturbations it is not surprising that some of the events are no longer stable, and will therefore not be seen in a flow field that is not subject to a constraint such as being irrotational or incompressible. Since the stable singularities in a general three-dimensional vector field are the fold, cusp, and swallowtail, we conclude that in the evolution of a two-dimensional field the events which alter the pattern of folds and cusps should be beak-to-beak, lips, and swallowtail. The results are illustrated by an example of the observed velocity field of sea ice drifting on the surface of the Arctic Ocean.

The notions of umbilic and antiumbilic points are generalised to arbitrary flow fields, where there is now no surface to which to relate them. These generalised umbilic and antiumbilic points occur in the general field of any symmetric tensor (strain-rate, strain, stress, for example), and fall into a natural extension (§ 5.2 and appendix 3) of the classification given by Berry and Hannay (1977) for the umbilic points of a surface. There are two new classes in addition to the four which Berry and Hannay described. Section 6 of the paper reviews some of the implications of the work and touches on possible applications.

2. Singularities in flow fields

A flow field is defined by a continuous vector function f which assigns to each point $\boldsymbol{x}$ in the 'source space' X a single velocity vector $\boldsymbol{u}$ in the 'target space' U (figure 1). We write

$$f: \quad \mathrm{X} \rightarrow \mathrm{U},$$

or, equivalently,

$$\boldsymbol{u} = f(\boldsymbol{x}).$$

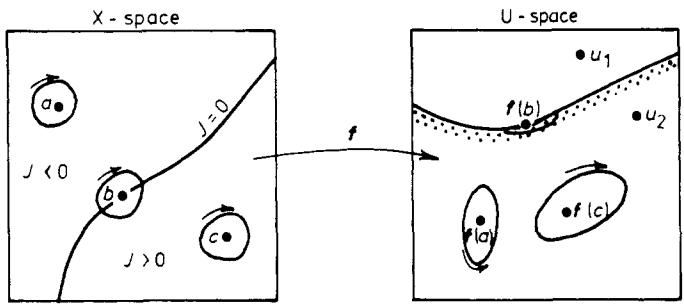

Figure 1. If the X-space is folded along the $J = 0$ line so that the upper left half is folded under the lower right, circuits around c will preserve their sense in U, circuits around a will reverse their sense, and circuits around b will degenerate. Points a and c are regular points because their neighbourhoods get mapped into neighborhoods in U. Point b is singular because its neighbourhood gets mapped degenerately into U. Point a is a J-negative point because the sense of a circuit about a gets reversed in U. Point c is a J-positive point. The point u_1 in U has no inverse images in X, while the point u_2 has two inverse images. As one moves across a fold in U-space from the unshaded to the shaded side, the number of inverse images increases by two.

For two-dimensional flows, we take X and U to be two-dimensional Euclidean spaces with the coordinates

$$\boldsymbol{x} = (x, y), \qquad \boldsymbol{u} = (u, v).$$

Thus each point (x, y) in physical space is mapped into a corresponding image point (u, v) in velocity space according to the flow velocity which exists at (x, y). We define $\mathbf{L}$ to be the velocity gradient matrix, and J to be the Jacobian of f:

$$\mathbf{L} = \begin{pmatrix} u_x & u_y \\ v_x & v_y \end{pmatrix}, \qquad J = \det \mathbf{L},$$

where subscripts denote differentiation. A point $\boldsymbol{x}$ is said to be *singular* if and only if the Jacobian J of f vanishes at $\boldsymbol{x}$. Points which are not singular are *regular*.

There is a geometric distinction between singular and regular points. Consider a small neighbourhood centred on a regular point $\boldsymbol{x}$. The image in U of this neighbourhood will be deformed by f as a circle is deformed into an ellipse. The Jacobian measures the ratio of the area of the image to that of the original neighbourhood. At singular points the image ellipse degenerates to a line segment (b in figure 1). The *sign* of $J(\boldsymbol{x})$ can also be interpreted in terms of a neighbourhood about $\boldsymbol{x}$. If a sense is given

to the perimeter of the neighbourhood in X, the image neighbourhood in U will have the same or opposite sense depending on whether $J(\boldsymbol{x})$ is positive or negative.

A theorem by Whitney (1955) states that the singular points of a function $f: \boldsymbol{R}^2 \rightarrow \boldsymbol{R}^2$ generically form *lines*. This can be seen intuitively by visualising the landscape whose height at any point $\boldsymbol{x}$ is $J(\boldsymbol{x})$. If we take $J = 0$ to be sea level, the coastlines are the sets of singular points. These lines separate regions where $J < 0$ from regions where $J > 0$.

2.1. Whitney's classification

Take any point $P = \boldsymbol{x}$ and consider the velocities of surrounding points relative to it. Thus, for the present purpose, P may be thought of as at rest. In short interval of time a small unit circle centred on P (figure 2(*a*)) will be deformed into an ellipse, a typical

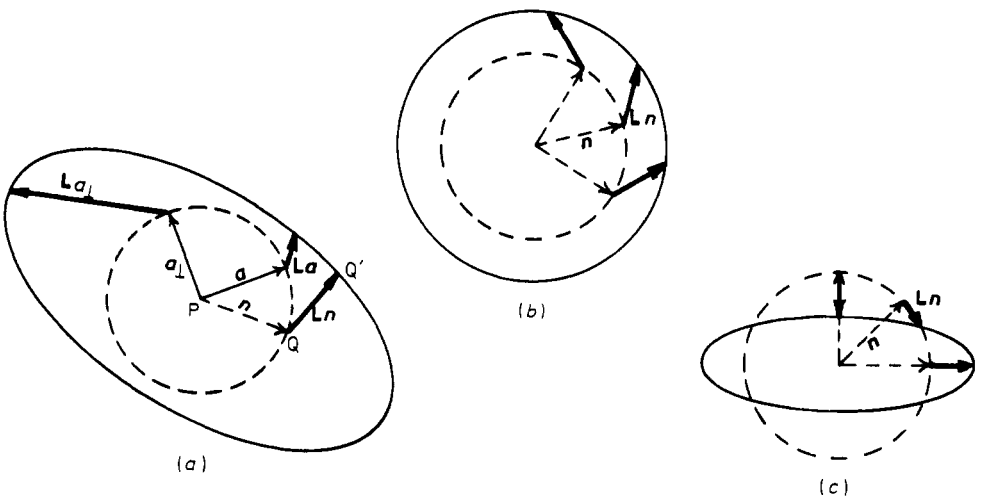

Figure 2. (*a*) The definition of $\boldsymbol{a}$ and $\boldsymbol{a}_\perp$. A unit circle deforms into an ellipse; $\mathbf{L}\boldsymbol{n}$ is the displacement of a point $\boldsymbol{n}$ on the unit circle. $|\mathbf{L}\boldsymbol{a}|$ is the minimum magnitude of displacement for all points on the unit circle; it occurs for the point given by $\boldsymbol{a}$. $|\mathbf{L}\boldsymbol{a}_\perp|$ is the maximum magnitude of displacement; it occurs for $\boldsymbol{a}_\perp$, normal to $\boldsymbol{a}$. Deformation of a unit circle at (*b*) an umbilic point and (*c*) an antiumbilic point (pure shear). In both cases the magnitude of the displacement $|\mathbf{L}\boldsymbol{n}|$ is independent of the direction of $\boldsymbol{n}$.

point Q moving to Q'. If PQ is the unit vector $\boldsymbol{n}$, since $\mathbf{L}$ is the velocity gradient, QQ' will be the vector $\mathbf{L}\boldsymbol{n}$. As $\boldsymbol{n}$ is varied, there will be one direction (and its opposite) that minimises $|\mathbf{L}\boldsymbol{n}|$; we call this special $\boldsymbol{n}$ direction $\boldsymbol{a}$ (only its direction rather than its sense will be significant). The perpendicular direction $\boldsymbol{a}_\perp$ maximises $|\mathbf{L}\boldsymbol{n}|$. It can be seen from figure 2(*a*) that, if there were no rotation, $\boldsymbol{a}$ and $\boldsymbol{a}_\perp$ would be simply the instantaneous directions of principal strain-rate, and $|\mathbf{L}\boldsymbol{n}|_{\max}$ and $|\mathbf{L}\boldsymbol{n}|_{\min}$ would be $|e_1|$ and $|e_2|$, where e_1 and e_2 denote principal strain-rates (this is less obvious when e_1 and e_2 have opposite signs). But the presence of rotation causes $|\mathbf{L}\boldsymbol{n}|$ to take different extreme values, and $\boldsymbol{a}$ and $\boldsymbol{a}_\perp$ are no longer the directions of principal strain-rate (they are in fact the principal directions of the matrix $\mathbf{L}^T\mathbf{L}$).

The special direction $\boldsymbol{a}$ has been used by Whitney (1955) to classify the singular points. He first showed that the loci of singular points in X are smooth lines, called *fold-lines*. At any point on a fold-line $|\mathbf{L}\boldsymbol{a}| = 0$. Special points called *cusp-points* exist

along a fold-line where $\boldsymbol{a}$ is tangent to the fold-line. In U the images of the fold-lines are lines, simply called *folds*, which have *cusps* at the images of the cusp-points.

Folds and cusps can be interpreted geometrically in terms of the graph of f. This graph is a (two-dimensional) surface G imbedded in four-dimensional X×U space (figure 3). (In fact in figure 3 the G surface is sketched in the three-dimensional space

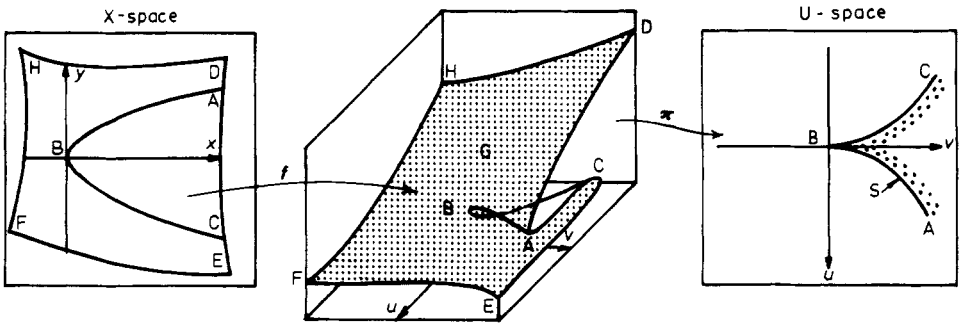

Figure 3. Folds and cusps in the velocity mapping f can be visualised as shown. The X-space, thought of as the stretchable sheet DEFH, is mapped into the three-dimensional space above (u, v) so that each point in X has a unique velocity (image) in U. This forms the graph G of the function f. The $J = 0$ line in X is labelled ABC. G is folded along this line. When G is projected by π into (u, v) space, the fold ABC in U has a cusp at B.

(u, v, y). We will discover below that locally $f: \boldsymbol{R}^2 \to \boldsymbol{R}^2$ always has the form $u = u(x, y)$, $v = x$ in suitable coordinates. Thus a point on the graph of f in X×U, i.e. a point (x, y, u, v) such that $(u, v) = f(x, y)$, can be represented by the point (u, v, y) where $u = u(x, y) = u(v, y)$—a point in $\boldsymbol{R}^3$.) Because f is single-valued, there is a one-to-one correspondence between points on G and points in X. But, with respect to U, G will be more complicated. 'Looking up' from a point $\boldsymbol{u}$ in U one might see several layers of the surface G, or none at all, corresponding to the number of points on G (and. therefore, in X) which have the velocity $\boldsymbol{u}$. The points $\boldsymbol{x}_i$, satisfying $\boldsymbol{u} = \boldsymbol{f}(\boldsymbol{x}_i)$, are the inverse images of $\boldsymbol{u}$ under f. As figure 3 illustrates, folds in the graph cause the number of inverse images to change. The projections of the folds in G into U are the folds in U. As one moves across a fold in U, the number of inverse images in X changes by two. Figure 3 also shows how two folds in the (u, v) plane can come together in a cusp. There are three inverse images for points inside the cusp but only one for points outside.

2.2. Relation to kinematic quantities

Since the classification of points on the basis of their Jacobian involves only first derivatives of the velocity field, it is related to the familiar quantities of divergence, shear and vorticity. In terms of quantities which are invariant under a rotation of coordinates in X, we define

$$\text{divergence} = d = u_x + v_y,$$

$$\text{shear} = s = +[(u_x - v_y)^2 + (u_y + v_x)^2]^{1/2},$$

$$\text{vorticity} = \omega = \tfrac{1}{2}(u_y - v_x).$$

Then the Jacobian satisfies

$$J = \tfrac{1}{4}(d^2 - s^2 + 4\omega^2).$$

Two special two-dimensional flows are of interest: incompressible and irrotational. In each case the two velocity components are determined by differentiation of a scalar function, namely, the *stream function* ψ or the *potential* ϕ:

$$\text{incompressible flow:} \quad u = \psi_y, \qquad v = -\psi_x;$$

$$\text{irrotational flow:} \quad u = -\phi_x, \qquad v = -\phi_y.$$

The scalar can be thought of as determining a surface whose height at the point (x, y) is ψ or ϕ and whose slope is everywhere small. The curvature of the surface is determined at each point by the symmetric 2×2 matrix of second partial derivatives, which has two principal values, the principal curvatures, $C_1 \geqslant C_2$. Observe that the Gaussian curvature $C_1 C_2$ (the determinant of this matrix) is equal to the Jacobian of the vector field $f: (x, y) \to (u, v)$:

$$J = C_1 C_2.$$

Furthermore, the direction $\boldsymbol{a}$ which minimises $|\mathbf{L}\boldsymbol{n}|$ and the perpendicular direction $\boldsymbol{a}_\perp$ which maximises $|\mathbf{L}\boldsymbol{n}|$ are identical with the directions of principal curvature of the ψ or ϕ surface. Table 1 shows the relation of $\boldsymbol{a}$ and $\boldsymbol{a}_\perp$ to the principal directions of strain-rate and to those fluid lines which are momentarily not rotating or not changing in length, and also the magnitudes of $|\mathbf{L}\boldsymbol{n}|_{\max}$ and $|\mathbf{L}\boldsymbol{n}|_{\min}$ in the two cases.

Special points exist on the ψ and ϕ surfaces where the $\boldsymbol{a}$ and $\boldsymbol{a}_\perp$ directions are not defined: $|\mathbf{L}\boldsymbol{n}|_{\max} = |\mathbf{L}\boldsymbol{n}|_{\min}$, or equivalently $|C_1| = |C_2|$. If $C_1 = C_2$ the point is called an *umbilic point*; if $C_1 = -C_2$ we call the point an *antiumbilic point.* At an umbilic point the surface is locally spherical; antiumbilic points are like symmetric saddle points, but with the tangent plane not horizontal. At these points, where the deformation of a unit circle is as in figures 2(*b*) and 2(*c*), the Jacobian matrix $\mathbf{L}$ has the forms:

umbilic point

$$\begin{pmatrix} a & b \\ -b & a \end{pmatrix}$$

antiumbilic point

$$\begin{pmatrix} a & b \\ b & -a \end{pmatrix}.$$

This characterisation does not depend on having the underlying surface ψ or ϕ. In general, we call points in a vector field satisfying $u_x - v_y = 0$ and $u_y + v_x = 0$ *generalised umbilic points.* Those satisfying $u_x + v_y = 0$ and $u_y - v_x = 0$ are *generalised antiumbilic points.* Special properties of the flow field in the vicinity of these points are given in table 1. Note that for irrotational or incompressible flow one of the conditions for antiumbilic points is satisfied everywhere. The remaining condition defines a *line* of antiumbilic points.

Under a suitable rotation of coordinates $\mathbf{L}$ at any point has the form

$$\mathbf{L} = \begin{pmatrix} e_1 & \omega \\ -\omega & e_2 \end{pmatrix},$$

where e_1 and e_2 are the principal values of strain-rate and ω is the vorticity. In terms of these quantities, the extreme values of $|\mathbf{L}\boldsymbol{n}|$ can be expressed as

$$|\mathbf{L}\boldsymbol{n}|^2_{\substack{\max \\ \min}} = \tfrac{1}{2}(e_1^2 + e_2^2) + \omega^2 \pm (e_1 - e_2)[\tfrac{1}{4}(e_1 + e_2)^2 + \omega^2]^{1/2}.$$

Table 1. The meanings of J, $\boldsymbol{a}$ and $\boldsymbol{a}_\perp$ in various flow fields.

	General flow field	Irrotational flow: potential function ϕ	Incompressible flow: stream function ψ
		$\omega = 0$, $u = -\phi_x$, $v = -\phi_y$	$e_1 = -e_2 = e \quad (e > 0)$ $u = \psi_y$, $v = -\psi_x$
	$\lvert\mathbf{L}\boldsymbol{n}\rvert_{\max}$, $\lvert\mathbf{L}\boldsymbol{n}\rvert_{\min}$	$\lvert e_1\rvert$, $\lvert e_2\rvert$	$\lvert e+\omega\rvert$, $\lvert e-\omega\rvert$
Principal directions of $\mathbf{L}^T\mathbf{L}$	$\boldsymbol{a}_\perp$, $\boldsymbol{a}$	Principal curvature directions of ϕ; parallel to fluid lines which are not rotating; principal directions of strain-rate	Principal curvature directions of ψ; parallel to fluid lines which are not altering in length; 45° to principal directions of strain-rate
Generalised umbilic point $\lvert\mathbf{L}\boldsymbol{n}\rvert_{\max} = \lvert\mathbf{L}\boldsymbol{n}\rvert_{\min}$ $J > 0$ Locus	Isotropic strain-rate $e_1 = e_2$ Point	Isotropic strain-rate, no rotation $e_1 = e_2$, $\omega = 0$ $\lvert\mathbf{L}\boldsymbol{n}\rvert = \lvert e_1\rvert = \lvert e_2\rvert$ Point	Pure rotation, no strain-rate $e = 0$, $\omega \neq 0$ $\lvert\mathbf{L}\boldsymbol{n}\rvert = \lvert\omega\rvert$ Point
Generalised antiumbilic point $\lvert\mathbf{L}\boldsymbol{n}\rvert_{\max} = \lvert\mathbf{L}\boldsymbol{n}\rvert_{\min}$ $J < 0$ Locus	Pure shear $e_1 = -e_2$, $\omega = 0$ Point	Pure shear $e_1 = -e_2$, $\omega = 0$ Line	Pure shear $e_1 = -e_2$, $\omega = 0$ Line
Singular point $J = 0$ $\lvert\mathbf{L}\boldsymbol{n}\rvert_{\min} = 0$ Locus	$\frac{1}{4}(d^2 - s^2 + 4\omega^2)$ $= e_1 e_2 + \omega^2 = 0$ Line	Uniaxial flow, no rotation $e_1 e_2 = 0$, $e_1 + e_2 \neq 0$ Line	Simple shear $e = \lvert\omega\rvert$ Line
$J \gtrless 0$ Locus	$d^2 + 4\omega^2 \gtrless s^2$ Region	$d^2 \gtrless s^2$ Region	$4\omega^2 \gtrless s^2$ Region

The conditions for generalised umbilic points and generalised antiumbilic points can now be stated as:

Generalised umbilic point		Generalised antiumbilic point	
$e_1 = e_2$,	ω arbitrary	$e_1 = -e_2$,	$\omega = 0$
isotropic strain-rate		pure shear	

These facts are summarised in table 1.

Consider the mapping $\boldsymbol{g}: \boldsymbol{R}^2 \to \boldsymbol{R}^2$, which takes $(x, y) \to (u_x - v_y, u_y + v_x)$. Points in X which are the inverse images of the origin are generalised umbilic points. The number of inverse images will change, always by two, when a fold of $\boldsymbol{g}$ passes through the origin in the target space. Thus, generically, generalised umbilic points can be created or destroyed only in pairs. A similar argument applies for the generalised antiumbilic points.

2.3. Examples of folds, cusps and umbilic points

Ice floating on the surface of the Arctic Ocean has a velocity field which, over distances of hundreds of kilometres, varies reasonably smoothly and continuously (§ 5.1). We use it as an example in figure 4(*a*), the velocity vectors being depicted at a grid of points in X-space by arrows. At each point the Jacobian can be evaluated, and, following a procedure described in appendix 2, the $J = 0$ lines (fold-lines) in X-space can be drawn. These are the heavy lines AB, CD, and EF in figure 4(*b*). The point A has position $(x, y) \approx (0, 150)$ km and velocity $(u, v) \approx (-1{\cdot}5, 4)$ cm s^{-1}. Mapping each point on the $J = 0$ lines in X-space into U-space in this way we obtain the image folds in U-space shown in figure 4(*c*).

At each point in X-space the ***a***-direction can be determined. Generalised umbilic and antiumbilic points are located where ***a*** is indeterminate. The ***a***-trajectories radiating from each of these points are sketched in figure 4(*b*). The general form of the entire set of ***a***-trajectories can be inferred from those drawn. A point of tangency

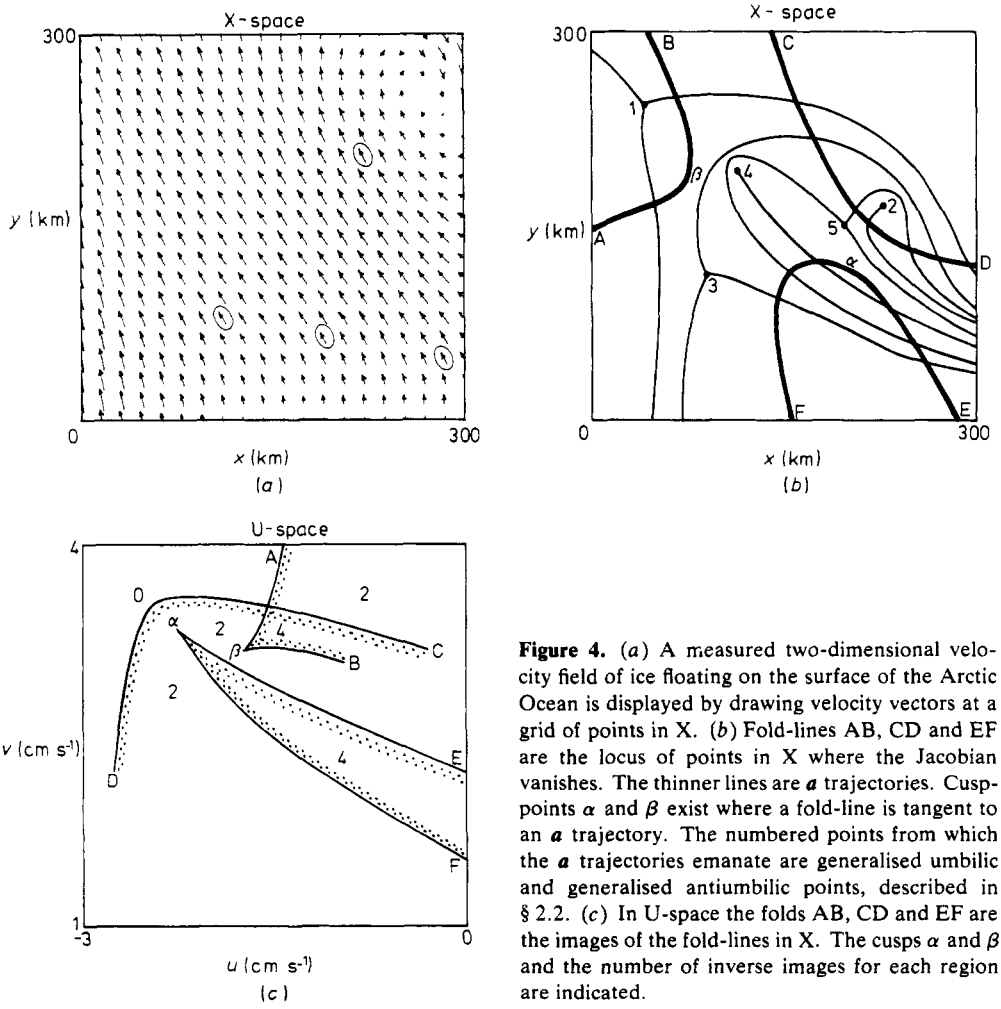

Figure 4. (*a*) A measured two-dimensional velocity field of ice floating on the surface of the Arctic Ocean is displayed by drawing velocity vectors at a grid of points in X. (*b*) Fold-lines AB, CD and EF are the locus of points in X where the Jacobian vanishes. The thinner lines are ***a*** trajectories. Cusp-points α and β exist where a fold-line is tangent to an ***a*** trajectory. The numbered points from which the ***a*** trajectories emanate are generalised umbilic and generalised antiumbilic points, described in § 2.2. (*c*) In U-space the folds AB, CD and EF are the images of the fold-lines in X. The cusps α and β and the number of inverse images for each region are indicated.

between an $\boldsymbol{a}$-trajectory and a $J = 0$ line determines a cusp in U-space. Two cusp-points, labelled α and β, exist in this field, and the corresponding cusps α and β in U-space are labelled accordingly.

The mapping from X to U can now be visualised as follows. Take the X-plane and fold it along the line CD. Then in the bottom sheet of the fold make a pleat at each of the points α and β. This is the basic geometry of the mapping.

The image space U is partitioned by the folds into regions where the number of inverse images differs, as indicated in figure 4(c); two new inverse images appear as one crosses to the shaded side of a fold. For example, a point 'inside' the EF fold has four inverse images, as indicated by the four circled vectors in figure 4(a). These four images can be imagined as brought into coincidence by successive foldings (and appropriate stretchings) of the X-plane.

2.4. Patterns of streamlines

Because the singularities we are discussing depend on the spatial derivatives of velocity, they reflect special patterns of strain-rate and rotation-rate. The velocity itself, as distinct from its derivatives, is irrelevant. However, a possible way of relating the singularities to readily visualised features of the velocity field is to consider the singular point in question to be at rest, and to ask what would then be the pattern of instantaneous streamlines in its neighbourhood. We confine the discussion to a few simple examples: the fold and the cusp in incompressible flow and in irrotational flow (see also Berry and Mackley 1977, and appendix 1).

The middle diagram of figure 5(a) shows the instantaneous streamlines for incompressible flow near the singular point in (x, y) when a fold lies along $v = 0$ in velocity space. The distinctive feature is the cusped streamline. v is always positive or zero, and it passes through its minimum value on the fold-line, shown as a broken line. Note that the flow at the centre (and indeed all along the fold-line) is simple shear. If the fold is now moved (right-hand diagram) to $v = -\epsilon$ (where $\epsilon > 0$), the origin in velocity space acquires two inverse images, and, accordingly, two stagnation points appear in the flow. If the fold is moved (left-hand diagram) to $v = +\epsilon$ there are no inverse images of zero velocity. Since the streamlines are perpendicular to $\nabla\psi$ (because $u = \psi_y$ and $v = -\psi_x$) they are contours of the stream function ψ. Figure 5(a) can then be usefully pictured as a series of contour maps of a ψ-landscape. The central map shows a valley whose slope is zero at one point, while the other two maps result from tilting the valley about the y axis (vertical in the diagram) first one way and then the other.

The two zeros (stagnation points) in the right-hand pattern are distinguished from one another by their *disclination index*. If one complete circuit is executed around the left-hand zero, the velocity vector rotates one revolution in the opposite sense to that of the circuit (index -1). In a similar circuit around the right-hand zero, the velocity vector rotates one revolution in the same sense (index $+1$). When zeros move, their indexes are preserved and when they interact the sum of their indexes is preserved; figure 5(a) is an example. A vortex has index $+1$ whichever way it rotates; so a vortex cannot be annihilated except by interaction with a zero of index -1 (saddle point in the ψ-landscape).

Figure 5(b) shows a set of possible streamline patterns where there is a cusp at and near the origin of velocity space. When the cusp moves to the left three zeros appear (total index -1), and when it moves to the right the three coalesce into a single

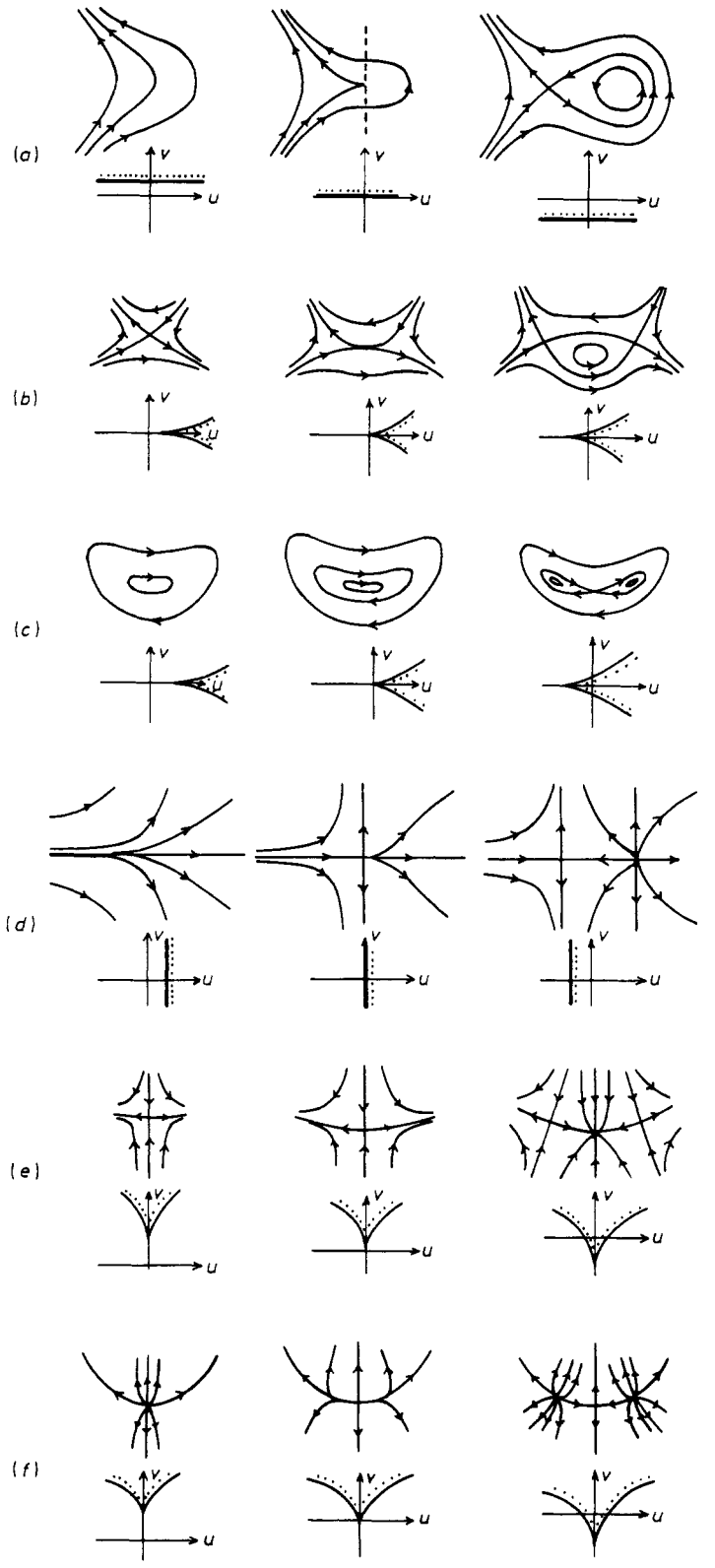

Figure 5. (*a*), (*b*), and (*c*): Patterns of instantaneous streamlines in X-space for incompressible flow. (*a*) shows how the streamlines change as a fold in velocity space (u, v) sweeps through the origin. In (*b*) and (*c*) a cusp in velocity space moves through the origin. (*d*), (*e*) and (*f*) are analogous patterns for irrotational flow. Whenever a fold or a cusp is near the origin of velocity space there will be a place in the flow field where the streamlines look like these patterns, distorted but topologically the same.

non-degenerate zero. Figure 5(*c*) shows another possible set of patterns corresponding to the same cusp; in this case the total index is always +1.

As a flow changes, the folds and cusps in velocity space will move. At special times a fold may sweep through the origin of velocity space, giving a change in the number of stagnation points; but a cusp, being a point in velocity space rather than a line, will never, generically, pass exactly through the origin. This has to be borne in mind when interpreting the patterns shown.

Analogous streamline patterns for irrotational flow are shown in figures 5(*d*), (*e*) and (*f*), They have been constructed by drawing the orthogonals to the streamlines in figures 5(*a*), (*b*) and (*c*) (which amounts to taking the contours of the potential function ϕ as those of the stream function ψ). Patterns of streamlines in incompressible flow are seen for the elliptic umbilic in Berry and Mackley (1977) and for the hyperbolic umbilic in Thom (1975, p. 77).

3. The evolution of a flow field

For time-dependent flow fields we expect the patterns of singularities to change with time, as illustrated, for example, in the sequences of figures 9(*a*), (*b*), and (*c*). Consider a one-parameter family of flow fields

$$\{f^t\colon \ \mathrm{X}\to\mathrm{U}\}, \qquad -\infty<t<\infty$$

where the superscript t labels each member of the family by the value of the parameter t, here thought of as time. The family can be visualised in terms of two decks of playing cards. In the first deck, labelled X, each card is a snapshot of X-space at a particular time. The second deck, labelled U, contains snapshots of U-space for the same sequence of times. The left-hand sides of figures 9(*a*), (*b*) and (*c*) are a sequence of cards from the X deck, the right-hand sides from the U deck. When the decks are stacked in order by time, they define three-dimensional spaces (x, y, t) and (u, v, τ), τ being simply the time label ($\tau = t$) for the second deck. The family of functions $\{f^t\}$ takes a point (x, y) from the t card of the X deck and assigns it to a point (u, v) on the $\tau = t$ card of the U deck. Thus, the family of functions $\{f^t\}$ is equivalent to a single function f from (x, y, t) into (u, v, τ) of the form

$$f\colon \ \boldsymbol{R}^3\to\boldsymbol{R}^3 \qquad \begin{aligned} u &= u(x, y, t),\\ v &= v(x, y, t),\\ \tau &= t. \end{aligned}$$

As in figure 9 each card in the U deck will have folds with cusps on them. Looking at the deck as the three-dimensional space (u, v, τ) the folds define surfaces—*fold sheets*—and the cusps define special lines in those surfaces appropriately called *ribs*. These fold sheets and ribs are the set S of singular points of the function $f\colon (x, y, t)\to(u, v, \tau)$ in precisely the same sense as we used the term singular for points in X. The point $(u_0, v_0, \tau_0) = f(x_0, y_0, t_0)$ is singular if the Jacobian of f vanishes at (x_0, y_0, t_0) or, equivalently, if the Jacobian of f^{t_0} vanishes at (x_0, y_0).

3.1. Events and stability

It is natural to ask whether there may be special points on the ribs. We shall see below that indeed there are. If (u_0, v_0, τ_0) is such a point, we say (u_0, v_0, τ_0) or (x_0, y_0, t_0) is

an *event*, that an event occurs at time t_0, and that these events determine the evolution of the field. We shall see that events can occur in two ways. At isolated points in (u, v, τ) space, singularities of higher order than the fold or the cusp can exist. The first type of event occurs as a sequence of planes $\tau =$ constant passes through the singularity. The second type of event occurs when a plane $\tau =$ constant is tangent to a rib.

Despite the great variety of flow fields which can occur, we wish to identify the short list of events which can occur in nature. To do this we exploit some recent mathematical results on stability.

This requires some mathematical definitions. Suppose f and g are two functions from $\boldsymbol{R}^n$ to $\boldsymbol{R}^n$. Then f and g are *equivalent* if there exist smooth and non-singular changes of coordinates $\eta: \boldsymbol{R}^n \to \boldsymbol{R}^n$ in the target space and $\zeta: \boldsymbol{R}^n \to \boldsymbol{R}^n$ in the source space such that $\eta \circ f = g \circ \zeta$. Strictly, equivalence is defined locally in the sense that the coordinate transformations must have non-zero Jacobian only in the neighbourhood of a point of interest. This definition of equivalence expresses the notion that the local *form* of a function does not depend on the particular choice of coordinates for the source and target spaces. One could obtain a narrower definition for equivalence by restricting the class of allowable coordinate changes: e.g. time-equivalence (Wassermann 1975). We choose throughout this paper to use the broadest definition. It is a matter of deciding how nearly congruent two objects must be in order to call them similar.

Also required now is the concept of a perturbation. Let $f: \boldsymbol{R}^n \to \boldsymbol{R}^n$, let ϵ be a small number, and let $\mathscr{C}$ be some class of functions from $\boldsymbol{R}^n \to \boldsymbol{R}^n$. Then $f + \epsilon h$ is a perturbation of f whenever h belongs to $\mathscr{C}$. The class $\mathscr{C}$ can be defined to admit very general perturbations to f or, if desired, only perturbations of a particular form.

A function $f: \boldsymbol{R}^n \to \boldsymbol{R}^n$ is said to be *stable* with respect to the class of perturbations $\mathscr{C}$ if for any h in $\mathscr{C}$, and small ϵ, the perturbed function $f + \epsilon h$ is equivalent to f. Physically, we expect any natural flow field to be subject to perturbations arising from fine details in the boundary and initial conditions which determine the flow, from the composition of the fluid itself, and from the limitations of the observation process. If the field is stable in this mathematical sense, the *form* of the field will not be altered by repeating the experiment or using a different observing technique—provided the perturbations to the field are small. This is why stable fields are of interest.

The notion of stability should be so chosen that all observed fields are stable. This requires that we satisfy two criteria:

(i) The class of perturbations used to define stability must be appropriate for the physical situation being studied and for the observation process.

(ii) It must be *generic* for a field to be stable, meaning that any field we encounter or construct (by picking polynomial representations for u and v, say) can be made stable (if it is not already) by a small perturbation.

For general flow fields (§ 5), we make the physical assumption that arbitrary perturbations to the evolving field are possible, thus taking the class $\mathscr{C}$ of perturbations to be the class of all smooth functions from $\boldsymbol{R}^3$ to $\boldsymbol{R}^3$. In this case, a result due to Mather (1971) implies that the stable functions are generic. This satisfies criterion (ii). However, one might argue that (i) is not satisfied—that, in fact, the only possible perturbations affect the velocity part but not the time part of $f: (x, y, t) \to (u, v, \tau)$. It can be shown, however, although we shall not prove it here, that this restriction of the class of perturbations (which alters the definitions of stability and genericity) does not alter the class of stable functions, nor change the fact that stable functions are generic.

When the nature of the flow is constrained by some special physics, the class of perturbations $\mathscr{C}$ may be restricted still more. If the fluid is incompressible, for example, $\mathscr{C}$ is restricted to the class of smooth functions satisfying $u_x + v_y = 0$. Since, in this case (which is treated in § 4), stability is defined with respect to a smaller class of perturbations, we expect to find a longer list of stable fields. The notion of a generating function (discussed in the next section) is useful for treating this case.

To summarise: our objective is to describe the observable events which occur naturally in the evolution of two-dimensional flow fields. To achieve this we first identify the appropriate class of perturbations. Next, we give a list of singular functions from $\boldsymbol{R}^3$ to $\boldsymbol{R}^3$ which are stable and generic with respect to that class of perturbations. This classifies the singularities in the sense that any singularity of a stable function is equivalent to one on the list. Then we describe the events which occur as we take sequences of time sections through the singularities.

3.2. Generating functions

Let Φ be a scalar function of x, y, u, v. In the catastrophe theory literature Φ would be called a potential, but we use the term generating function, having already used potential in a different sense. Identifying the coordinates x, y as *state* variables and u, v as *control* variables, we impose the condition that, for given values of the control variables, Φ should be stationary with respect to the state variables; that is, the gradient of Φ with respect to the state variables must vanish. For a given point (u, v) in control space the gradient condition defines the associated stationary points of Φ in state space (x, y). There may be zero, one or several of these. As the point in control space moves, so the stationary points in state space also move, and for certain points in control space two or more of them may coalesce to form degenerate stationary points. The basic theorem in catastrophe theory classifies the sets of singular points in control space for which this happens. With two control variables, as here, the singular sets are either fold lines or cusp points. These are structurally stable in the sense that a small perturbation of the generating function leaves their local structure intact: the perturbed and unperturbed singular sets can be related by a smooth, reversible change of coordinates.

The stationary condition on Φ associates certain points in (x, y) with a given point in (u, v), but not necessarily vice versa: in general, fixing (x, y) may not determine (u, v). Since in our application each point (x, y) must have a unique velocity, we must make sure that any generating function we use has this property. For steady irrotational flow with potential ϕ a suitable generating function would be

$$\Phi(x, y; u, v) = \phi(x, y) + ux + vy$$

for $\Phi_x = \Phi_y = 0$ implies

$$u = -\phi_x, \qquad v = -\phi_y.$$

For steady incompressible flow with stream function ψ we can take

$$\Phi(x, y; u, v) = \psi(x, y) - uy + vx$$

for $\Phi_x = \Phi_y = 0$ implies

$$u = \psi_y, \qquad v = -\psi_x.$$

For time-dependent irrotational and incompressible flows t may be regarded simply as a parameter. Thus the one-parameter family of generating functions $\Phi(x, y; u, v; t)$ generates the one-parameter family of flow functions $\{f^t\}$. An alternative is to construct a generating function Φ for $f: \boldsymbol{R}^3 \to \boldsymbol{R}^3$ involving (x, y, t) as state variables and (u, v, τ) as controls, as follows. Define

$$\Phi(x, y, t; u, v, \tau) = \begin{cases} \phi(x, y; \tau) + ux + vy + \frac{1}{2}t^2 - \tau t & \text{(irrotational)} \quad (1) \\ \psi(x, y; \tau) - uy + vx + \frac{1}{2}t^2 - \tau t & \text{(incompressible).} \quad (2) \end{cases}$$

Then $\Phi_x = \Phi_y = \Phi_t$ implies

$$u = -\phi_x, \qquad v = -\phi_y, \qquad \tau = t \qquad \text{(irrotational)}$$

$$u = \psi_y, \qquad v = -\psi_x, \qquad \tau = t \qquad \text{(incompressible)}$$

as required.

4. Singularities which are stable with respect to perturbations of Φ

Suppose f is an irrotational or incompressible time-dependent two-dimensional flow field and is derived from a generating function of the form (1) or (2). The singularities of f which are stable with respect to perturbations of Φ are given by Thom (1975) as the fold, cusp, swallowtail, hyperbolic and elliptic umbilic catastrophes.

There is a technical point here. By restricting our attention to irrotational or incompressible flows, we have, in effect, required that the singularities be stable with respect to perturbations of ϕ or ψ. This is the natural physical assumption (criterion (i)). Thom's work, however, applies when the singularities are stable with respect to perturbations of the generating function Φ. With respect to our smaller class of perturbations it is conceivable that there are additional stable singularities; but it is unlikely since the observational evidence from both flow fields and optical caustics (§ 4.3) gives no suggestion of it.

Recall that in $\boldsymbol{R}^3$ the folds form sheets, and the cusps lines (called ribs). The swallowtail, hyperbolic and elliptic umbilic singularities are points in $\boldsymbol{R}^3$. Each of these points is caused by a special intersection of fold sheets and ribs as illustrated in figure 6. Events occur when a τ section contains one of these special points. Events also occur when a τ section is tangent to a curved rib; in a sequence of τ sections the number of cusps will then change by two. This can happen in two ways—beak-to-beak, and lips—as illustrated in figures 8(c) and 8(d).

One has to imagine the singular sets of figure 6 distorted and placed in various orientations in the control space (u, v, τ). In the usual form of catastrophe theory, all the control variables are on an equal footing; one can transform freely between them and the singular sets can have any orientation. But when (u, v, τ) are taken as controls it is necessary to maintain a distinction between time τ and the other two variables. This has the effect, as we shall see, of restricting the possible orientations of the singular sets, and therefore the possible sections of them by the 'observation plane' τ = constant.

Table 2 gives standard forms (Poston and Stewart 1976) for the generating function for the five elementary catastrophes having up to three control variables (a, b, c). Since the number of essential state variables is less than three, we have included terms in Y^2 and Z^2, which do not produce singularities, to make the state

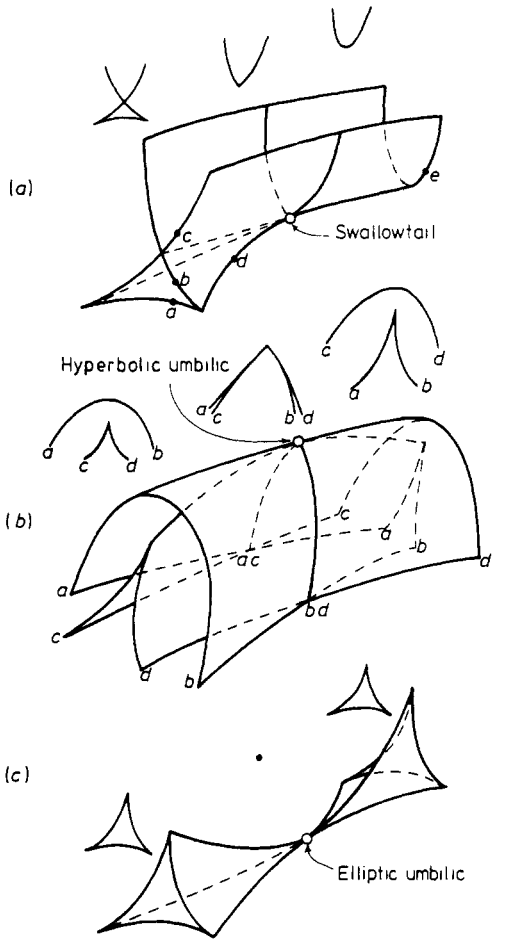

Figure 6. (*a*) Swallowtail, (*b*) hyperbolic umbilic and (*c*) elliptic umbilic catastrophes. The surfaces shown are the singular sets in control space (a, b, c). Sections are given for $a < 0$, $a = 0$ and $a > 0$.

variables (X, Y, Z). A generating function (1) or (2) for an irrotational or incompressible flow having one of these singularities must be transformable into the appropriate standard form. For this purpose both the state and the control variables can be transformed by arbitrary smooth reversible coordinate changes; the transformations for the state variables can include the control variables as parameters (because these are held constant when applying the gradient condition) but not vice versa. Thus the coordinate transformations are

$$(X, Y, Z) \leftrightarrow (x, y, t; a, b, c),$$

$$(a, b, c) \leftrightarrow (u, v, \tau),$$

and the form of (1) and (2) ensures that $t = \tau$.

An example of an irrotational or incompressible flow with a *fold* singularity is produced by choosing the upper signs in the standard form from table 2 and first

Table 2.

Singularity	Generating function
Fold (surface in $\boldsymbol{R}^3$)	$X^3 + aX \pm \frac{1}{2}Y^2 \pm \frac{1}{2}Z^2$
Cusp (line in $\boldsymbol{R}^3$)	$X^4 + aX^2 + bX \pm \frac{1}{2}Y^2 \pm \frac{1}{2}Z^2$
Swallowtail (point in $\boldsymbol{R}^3$)	$X^5 + aX^3 + bX^2 + cX \pm \frac{1}{2}Y^2 \pm \frac{1}{2}Z^2$
Hyperbolic umbilic (point in $\boldsymbol{R}^3$)	$X^3 + Y^3 + aXY + bX + cY \pm \frac{1}{2}Z^2$
Elliptic umbilic (point in $\boldsymbol{R}^3$)	$X^3 - 3XY^2 + a(X^2 + Y^2) + bX + cY \pm \frac{1}{2}Z^2$

transforming the state variables

$$(X, Y, Z) = (x, y + b, t - c)$$

to give

$$\Phi = x^3 + \tfrac{1}{2}y^2 + ax + by + \tfrac{1}{2}t^2 - ct, \tag{3}$$

ignoring terms in control variables only, which are irrelevant to the gradient condition. Then, comparing with the forms (1) and (2), we recognise that the transformations of the control variables

$$(a, b, c) = (u, v, \tau) \text{ or } (v, -u, \tau)$$

give ϕ or $\psi = x^3 + \frac{1}{2}y^2$. Thus for the irrotational case we have the steady flow $u = -3x^2$, $v = -y$, $\tau = t$.

Another choice of control variables $(a, b, c) = (u + \tau, v, \tau)$ gives the time-dependent irrotational flow $u = -3x^2 - t$, $v = -y$, $\tau = t$. In this case the fold in (x, y) is stationary at $x = 0$, but in the observation plane (u, v) there is a moving fold parallel to the v axis.

In the three-dimensional control space (u, v, τ) a fold sheet can never be tangent to the observation plane. To see this, note that the fold sheet is $a = 0$, and so, if it were tangent to (u, v) we should have $a = \tau$. To obtain $\tau = t$ from (3) we must put $c = \tau$; but these two results together make the Jacobian of the transformation $(a, b, c) \rightarrow (u, v, \tau)$ vanish, and so the result follows.

To obtain examples of a *cusp* (rib) from the standard form in table 2, take

$$(X, Y, Z) = (x, y - x^2 + a, t - c),$$

$$(a, b, c) = (v, u, \tau) \qquad \text{or} \qquad (-u, v, \tau).$$

This gives

$$\phi \text{ or } \psi = \tfrac{3}{2}x^4 - x^2 y + \tfrac{1}{2}y^2.$$

Since this expression does not involve τ, the rib is perpendicular to the observation plane. In a more general situation, a rib can intersect the observation plane at any

angle. Or it may have a point of tangency with the observation plane to give the beak-to-beak or lips events, but the contact of the rib must not be such that its associated fold sheets also become tangent to the (u, v) plane.

For the *swallowtail* use the standard form in table 2 and the coordinate transformations

$$(X, Y, Z) = (x, y - x^2 + b, t - a)$$

$$(a, b, c) = (\tau, v, u) \qquad \text{or} \qquad (\tau, -u, v)$$

which, after neglecting x^5 for small x, give

$$\phi \text{ or } \psi = \tfrac{1}{2}x^4 - x^2 y + \tfrac{1}{2}y^2 + \tau x^3.$$

Alternatively, one could take

$$(X, Y, Z) = (x, y - x^3 + a, t - b)$$

$$(a, b, c) = (v, \tau, u) \qquad \text{or} \qquad (-u, \tau, v)$$

giving

$$\phi \text{ or } \psi = x^5 - x^3 y + \tfrac{1}{2}y^2 + \tau x^2.$$

A sequence of τ sections for the first case ($\tau = a$) is shown in figure 6(a) and for the second case ($\tau = b$) in figure 7(a). These sections are special. If τ is identified with a linear combination of a and b, the τ sections intersect the singular set more generally. For example, the sequence in figure 7(b) shows a cusp and fold; then the section passes through the swallowtail point and two new cusps form; one of them annihilates the original cusp in a beak-to-beak event and finally the other cusp moves away. (The same sequence was inferred in the sections of light caustics reported by Berry and Nye (1977)).

Note that in the swallowtail we cannot equate τ with c and still get Φ into form (1) or (2). This implies that the swallowtail plane (horizontal in figure 6) cannot be tangent to the 'observation plane'. As confirmation notice that, if it were, fold sheets would become tangent to the observation plane, and we have already seen that this is impossible.

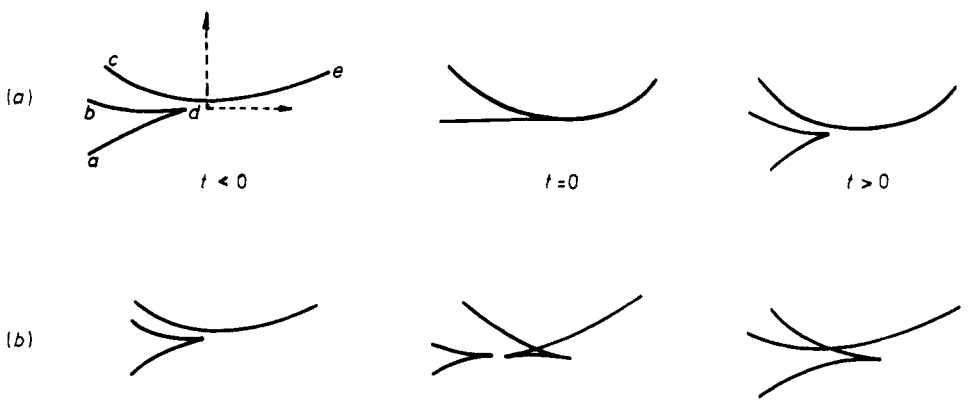

Figure 7. (a) A special sequence of sections of the swallowtail holding b constant in each section (see table 2). The labelled points correspond to points in the swallowtail of figure 6. (b) A general sequence of the swallowtail holding a linear combination of a and b constant.

Examples of flow fields containing *umbilic events* are

$$\phi \text{ or } \psi = \begin{cases} x^3+y^3+\tau xy & \text{(hyperbolic umbilic)} \\ x^3-3xy^2+\tau(x^2+y^2) & \text{(elliptic umbilic).} \end{cases} \tag{4}$$

In these cases τ has to be identified with a, so the (u, v) plane always gives the sections sketched in figure 6. However, in general, b and c will involve τ as well as u and v, so that successive time sections will show a drift across the (u, v) plane.

In constructing flow fields from generating functions we have considered only coordinate transformations which produce forms (1) or (2). This is because of the physical interest in irrotational and incompressible flows. But time-dependent two-dimensional flows can readily be constructed from generating functions with neither form (1) nor (2). For example, the cusp function

$$\Phi = \tfrac{1}{4}x^4+\tfrac{1}{2}vx^2-ux+\tfrac{1}{2}y^2-vy$$

generates the flow $u = x^3+xy$, $v = y$, which is neither irrotational nor incompressible. The results of this section would still apply provided the flow is stable with respect to perturbations of the generating function. Perhaps there are physical situations where this is the case; if so, the authors would be glad to learn of them.

4.1. The geostrophic flow of the atmosphere

In the geostrophic approximation the horizontal flow of the free atmosphere is an example of incompressible flow. Here the flow is determined by a balance between the pressure-gradient force and the Coriolis force, which is proportional to the velocity and acts at right angles to it. If $p(\boldsymbol{x})$ is the pressure, then

$$u = \Omega\frac{\partial p}{\partial y}, \qquad v = -\Omega\frac{\partial p}{\partial x},$$

where Ω may be considered constant over the small ranges of latitude we shall be considering. Thus Ωp plays the part of a stream function ψ in incompressible flow.

Albright (1977) has fitted a sixth-order polynomial in x and y at six-hour intervals to a set of pressure measurements. For several of his fields we have determined the $J = 0$ lines in (x, y) space and the corresponding folds and cusps in (u, v) space. The fields in figure 9 have enough continuity in time to be interpreted as a sequence of sections through the fundamental catastrophes.

In (x, y) space we have sketched the directions $\boldsymbol{a}$ which minimise $|\mathbf{L}\boldsymbol{n}|$, the antiumbilic lines, where the $\boldsymbol{a}$ directions turn through 90°, and the umbilic points. Since the J-positive regions can be identified in each figure, we have labelled them and the images of their boundaries in (u, v). They form islands in X where vorticity dominates shear ($2|\omega| > s$). The total J-positive and J-negative areas are roughly equal (within a factor of two, say) and so we can expect that the $J = 0$ level will more frequently pass near saddle points in the J surface than near local extremes. The hyperbolic umbilic catastrophe occurs when J vanishes at a saddle in the J surface (figure 8(a)). The elliptic umbilic occurs when J vanishes at an extreme (figure 8(b)). Therefore, we expect to find more hyperbolic umbilic events than elliptic umbilic events.

The sequence in figure 9 contains a good example of a hyperbolic umbilic catastrophe. Observe the regions labelled A and D at each of the three times. The two

positive regions move together sandwiching an antiumbilic line between them. Initially, the U image shows the fold corresponding to A to have a cusp 'inside' the smooth fold corresponding to D (see the sections of the hyperbolic umbilic catastrophe sketched in figure 6). Region A also has an umbilic point. The second sketch is very close to the critical time. Regions A and D meet at the antiumbilic line. The images in U have a common finite angle here (not a cusp), and A has lost its umbilic point. In the last of the sequence, A's image has moved across D's, and is no longer cusped at this place. The umbilic point is now in D. Antiumbilic lines separate regions where the total curvature C_1+C_2 of the stream function surface has opposite sign; thus regions A and D can never merge.

In this example and in others of the same sort, there is no shortage of folds or cusps (surprisingly, in view of the superficial appearance of smoothness in the vector fields). Hyperbolic umbilic catastrophes are seen in sequences of images and we have observed sections suggestive of the elliptic umbilic catastrophe. We have not observed the swallowtail in our (limited) study of the geostrophic wind. Over a longer time we should expect to see regions losing their identity through beak-to-beak events (Figure 8(*d*)) (between regions B and D, say, because they are not separated by an antiumbilic line). And we should see doubly-cusped regions like C simply appear or disappear by lips events (figure 8(*c*)).

4.2. Classification of umbilic points

The umbilic points of a surface, such as the ψ surface, where it is locally spherical, may be classified in three different ways, which are interrelated in a way recently described by Berry and Hannay (1977) and shown in table 3. The first classification depends on the *disclination index*, already introduced in § 2.4 in relation to the directions of a vector field near a zero, but now applied instead to the directions of curvature of a surface near an umbilic point. The index of the umbilic point is $\pm\frac{1}{2}$ according to whether the principal curvature directions rotate by $\pm\pi$ during a circuit around the point. Consider, for example, the upper of the two umbilic points in region C of figure 9(*b*), and recall that the $\boldsymbol{a}$ lines shown are the same as one of the two sets of curvature lines of ψ. In a clockwise circuit the $\boldsymbol{a}$ direction rotates by π clockwise, and so the index is $+\frac{1}{2}$. On the other hand, in a clockwise circuit around the other umbilic point in C the $\boldsymbol{a}$ direction rotates by π anticlockwise, and so the index of this point is $-\frac{1}{2}$.

Figure 10 shows the three possible patterns, called by Berry and Hannay star (S), lemon (L) and monstar (M). Note that S and M each have three straight $\boldsymbol{a}$ lines emanating from the umbilic point, while L has one. Here, in § 5.2, and in appendix 3, we replace Berry and Hannay's SLM pattern classification with a three or one *line* classification depending on the number of straight $\boldsymbol{a}$ lines meeting the umbilic point.

The *contour* classification (called the catastrophe classification by Berry and Hannay) depends on the envelope of normals to the ψ surface (its 'focal surface'): elliptic (E) if the focal surface is as in figure 6(*c*), and hyperbolic (H) if it is as in figure 6(*b*). This is equivalent to a distinction, more relevant to our present purpose, based on the forms of the contours of constant principal curvatures, C_1 and C_2, of the surface near the umbilic point: for E both sets of contours are ellipses; for H both sets are hyperbolas. (Refer to figures 8(*a*) and (*b*) at, say, $t<0$. Since C_1 is defined as always the greater of the two principal curvatures, the C_1 and C_2 surfaces form a cone. Therefore the sections of constant C_1 (and C_2) are hyperbolas in figure 8(*a*) and ellipses in figure 8(b).)

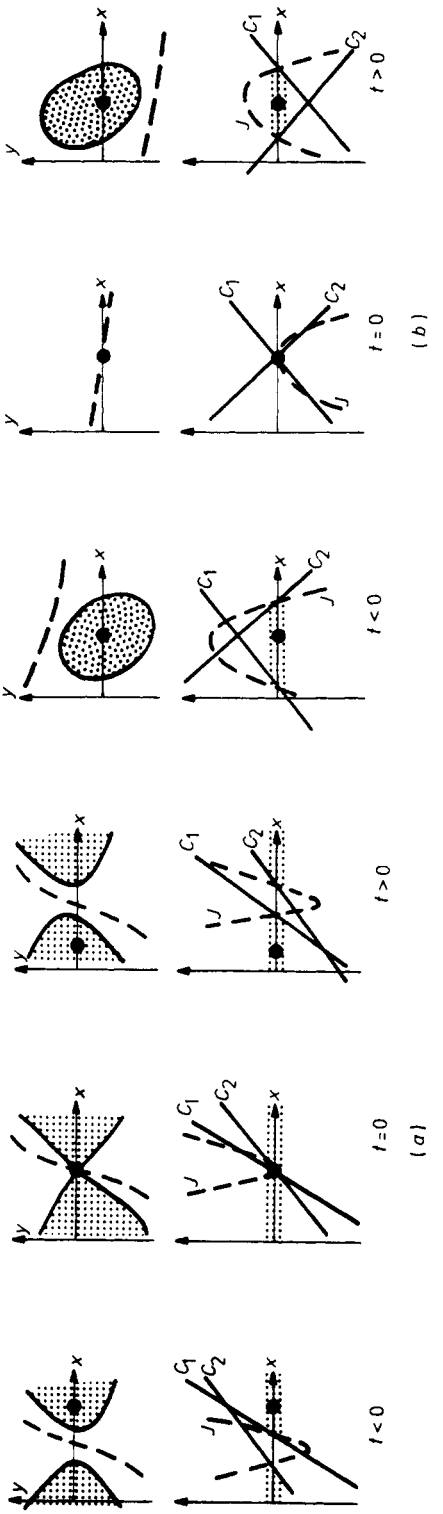
x
y
C_1
C_2
J
$t > 0$
$t = 0$
(b)
$t < 0$
$t > 0$
$t = 0$
(a)
$t < 0$

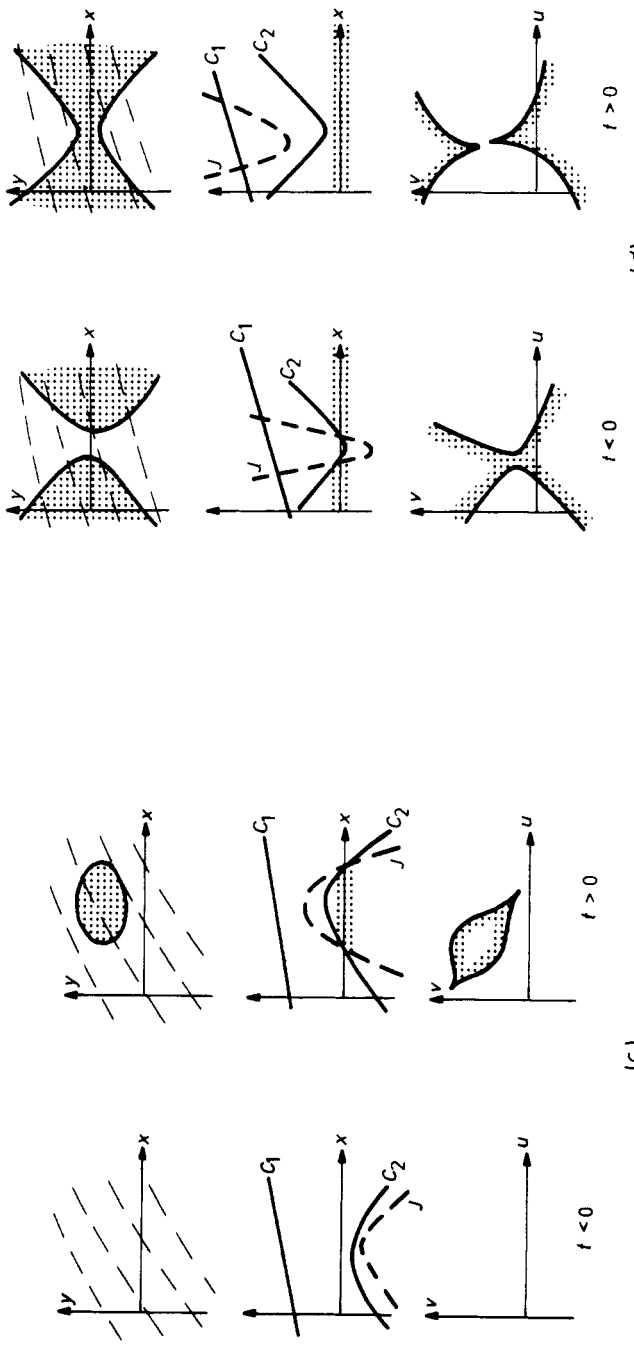

Figure 8. The principal curvatures C_1 and $C_2 (C_2 \geqslant C_2)$ of the stream or potential function plotted against x. Zeros in C_1C_2 determine the fold-lines; zeros in $C_1 - C_2$ are umbilic points (●); zeros in $C_1 + C_2$ are antiumbilic lines. When the condition for a fold-line is satisfied at an umbilic point ($C_1 = C_2 = 0$) an umbilic catastrophe occurs, either hyperbolic (*a*) or elliptic (*b*). On the other hand, lips (*c*) and beak-to-beak (*d*) events do not involve umbilic points. In (*a*) and (*b*) the bold broken curve in (x, y) is an antiumbilic line. Shading indicates regions where $J > 0$. In (*c*) and (*d*) the broken curves in (x, y) are $\boldsymbol{a}$-trajectories. (These sketches are not complete analyses of the events; in general, the curvatures are functions of both x and y.)

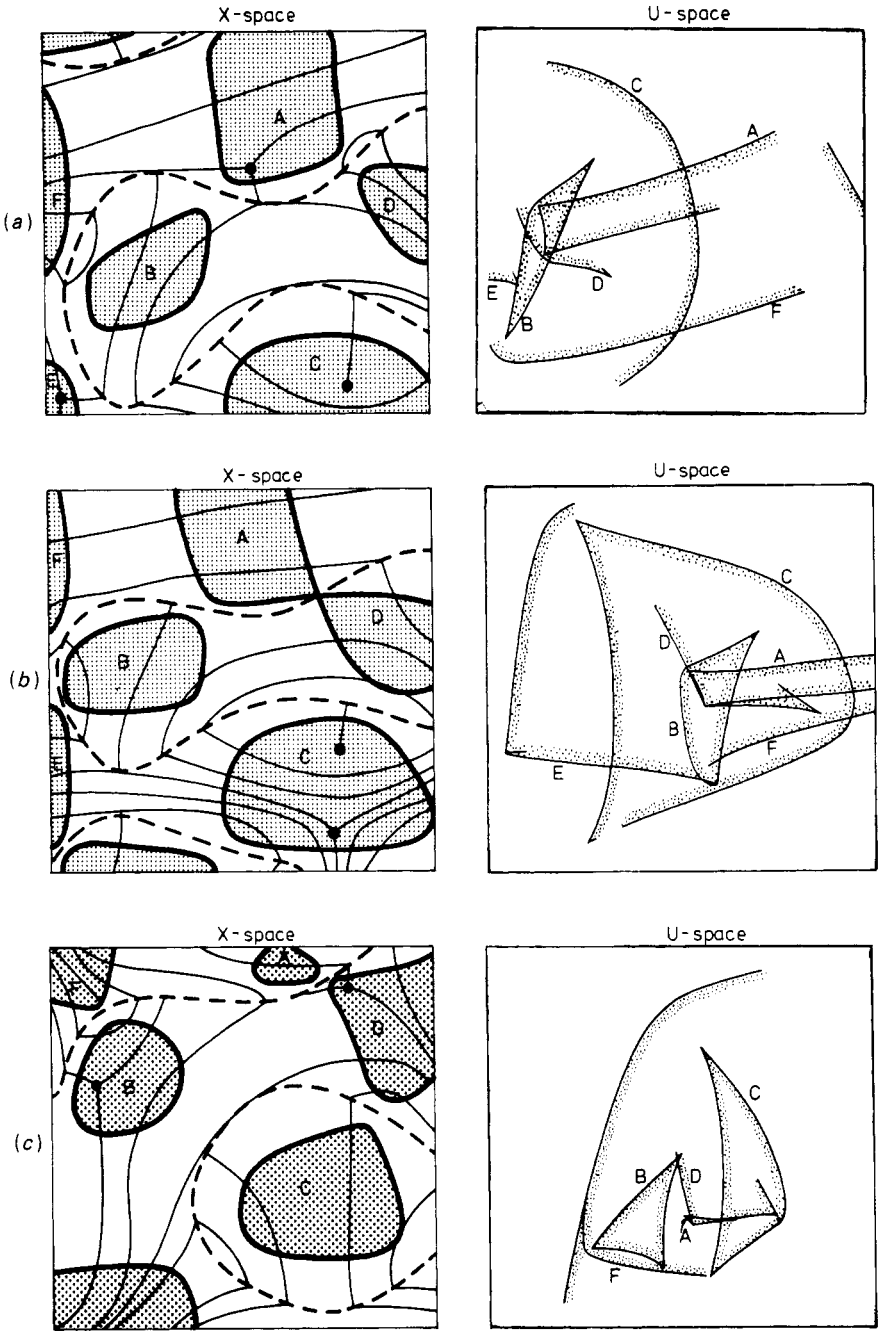

Figure 9. Analysis of singularities in the geostrophic wind field, for an 18-hour period in July 1975 over the Beaufort Sea. (*a*) 8 July 1975, 12 00 GMT; (*b*) 8 July 1975, 18 00 GMT; (*c*) 9 July 1975, 00 00 GMT. The X-space measures 1125 km on each side. The full variation in U-space is about 20 m s^{-1}. The heavy full curves in X-space are $J = 0$ lines. The regions of positive J are shaded and lettered. The broken curves are antiumbilic lines and the thin full curves are $\boldsymbol{a}$-trajectories. Solid dots mark umbilic points. The lines in U-space are the images of the $J = 0$ lines (fold A being the image of the boundary of region A, and so on).

Table 3. Classification of umbilic points (Berry and Hannay 1977).

Index	$-\frac{1}{2}$	$+\frac{1}{2}$
Line	3	1
Contour	E	H
Pattern	S	M L

(S) star, (M) monstar, (L) lemon,
(E) elliptic, (H) hyperbolic

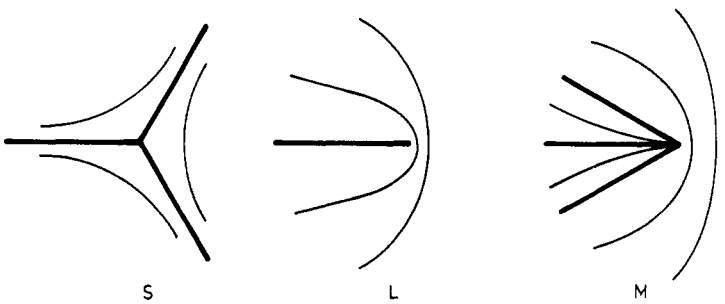

Figure 10. Pattern classification for (S) star, (L) lemon and (M) monstar. The direction lines for $\boldsymbol{a}$ are shown. (The reason for the word lemon is revealed by drawing the orthogonal set of $\boldsymbol{a}_\perp$ as well.)

There is a possible source of confusion here. The catastrophes we deal with in this paper are all associated with points in the flow field where $J = 0$; therefore, the umbilic points are not catastrophes in our sense unless they happen to move on to the $J = 0$ line. Our catastrophes are thus different from those referred to in the catastrophe classification of umbilic points. However, if a hyperbolic umbilic point comes on to the $J = 0$ line it does produce a hyperbolic umbilic catastrophe in our sense, as recognised by its pattern of folds in velocity space; and similarly if a $J = 0$ line collapses on to an elliptic umbilic point it produces an elliptic umbilic catastrophe in our sense.

If we consider the three two-fold distinctions (index, number of lines, and contour) there are 2^3 possible categories, but four of them are empty because they demand incompatible conditions. The remaining four can be symbolised as:

$$-3\text{E(star)} \qquad -3\text{H(star)} \qquad +3\text{H(monstar)} \qquad +1\text{H(lemon)}.$$

Table 3 is a one-dimensional Venn diagram showing the overlaps between the classifications of umbilic points. To illustrate by example (but see the proviso below), in figure 9(*a*) the umbilic point in region A is (−3H); H and not E because the point later passes over to region D during a hyperbolic umbilic event. The upper umbilic point in C (figure 9(*b*)) is (+3H) or (+1H) because it has positive index (higher magnification would be needed to resolve the pattern). The lower umbilic point in the same region is (−3H); we assign H because it annihilates the upper point and only H's

can annihilate (appendix 3). In figure 9(*c*) we have already identified the umbilic point in D as (−3H). The umbilic point in B is also (−3H); H not E because B has acquired a single umbilic point, and we believe it can only do this by a hyperbolic catastrophe (involving interaction with a neighbouring region). Proviso: these attributions assume that the points retain their classification as the field evolves with time (we shall see, however, in appendix 3 that transitions from one class to another are possible).

4.3. Analogy with geometrical optics

There is a direct analogy between the singularities of an irrotational or incompressible flow field and certain patterns of light caustics in geometrical optics. For example, if the reader places his eye close to raindrops on a window pane and views a distant light through them, the pattern of directional caustics seen at infinity, with its bright folds and cusps, will be strikingly similar to a pattern of singularities in velocity space.

To establish the analogy, start with a piece of wavefront in the plane $z = 0$ and perturb it slightly from the plane by an amount $F(x, y)$ (for example, by passing a plane wave through a sheet of uneven glass). The perturbation deflects the rays from the z direction so that they strike a screen 'at infinity' in points which can be labelled by coordinates (ξ, η), where

$$\xi = -\frac{\partial F}{\partial x}, \qquad \eta = -\frac{\partial F}{\partial y}.$$

Thus the rays make a gradient mapping from the wavefront space (x, y) to the screen (ξ, η). For irrotational flow the analogy is

$$\phi(x, y) = F(x, y), \qquad u = \xi, v = \eta;$$

for incompressible flow it is

$$\psi(x, y) = F(x, y), \qquad u = -\eta, v = \xi.$$

The time-development of the singularities in (u, v) space of a velocity field therefore corresponds exactly to the changing pattern of caustics at infinity as the initial wavefront is allowed to change.

If the perturbed wavefront is produced by passing the light not through a sheet of glass, which might have any thickness pattern, but through, say, an irregular water droplet whose form is governed by surface tension, there is a constraint on the form of the wavefront: if the effect of gravity is negligible, the sum of the principal curvatures of the wavefront has to be constant. This, in turn, restricts the forms of the caustics (Berry 1976, Nye 1978). The analogy for irrotational flow would be a flow with a uniform density of source strength. For incompressible flow the constraint would be uniform vorticity.

5. Singularities which are stable with respect to perturbations of f

Consider, as in § 3, an evolution of a map from $\boldsymbol{R}^2$ to $\boldsymbol{R}^2$. Singularities which (in § 4) were stable with respect to perturbations of an underlying generating function may not be stable under a more general perturbation of the vector field. For example, consider the vector function form of the hyperbolic umbilic $u = x^2 + ty$, $v = y^2 + tx$

(obtained from the expression for ϕ in (4) after suitable scalings). The condition $J = 0$ which defines the fold-lines in (x, y) space can be written

$$4xy - t^2 = 0.$$

This defines a family of hyperbolas in (x, y) space which contains a degenerate hyperbola when $t = 0$ (compare figure 8(a)).

Suppose that f is perturbed to be

$$u = x^2 + ty + \epsilon y, \qquad v = y^2 + tx - \epsilon x.$$

The condition $J = 0$ now defines two degenerate hyperbolas at $t = \epsilon$ and $t = -\epsilon$. In fact, as seen by the coordinate changes indicated in figure 11(b), each of the points $(x = y = 0, t = \pm\epsilon)$ is a swallowtail (figure 11(a)). Thus, under a perturbation which

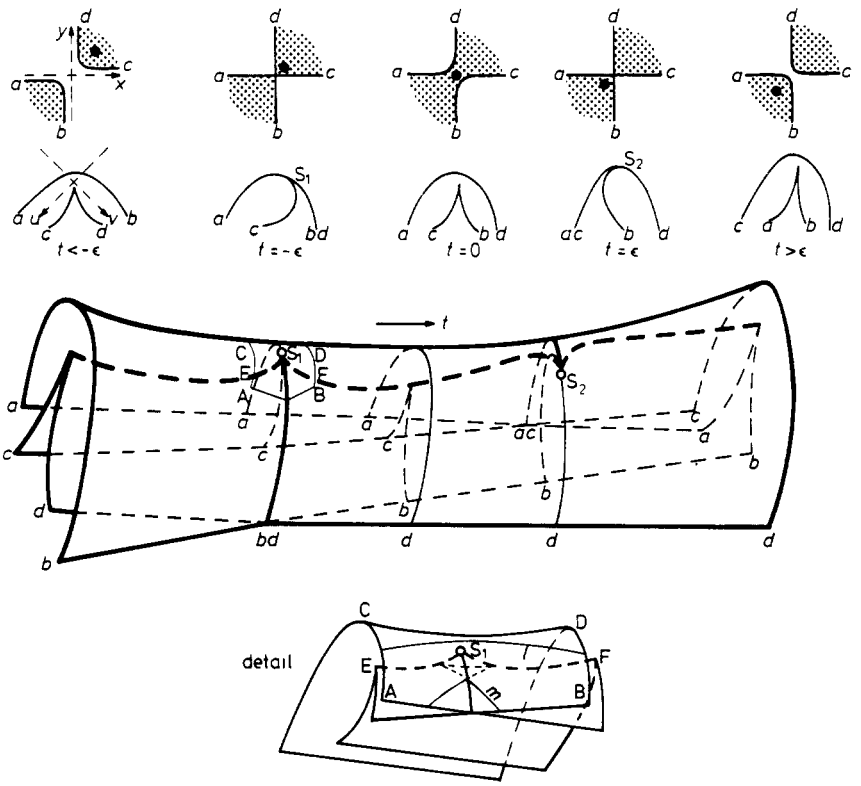

Figure 11. (a) The perturbed hyperbolic umbilic catastrophe. The mapping $u = x^2 + (t + \epsilon)y$, $v = y^2 + (t - \epsilon)x$ has swallowtail events S_1, S_2 at $t = \pm\epsilon$. The sequence of t sections is topologically equivalent to the sections of the swallowtail 'from the side,' in figure 6. One can see the swallowtail in the detail of the region containing S_1. The key to recognising the swallowtail (see figure 6) is to identify the two ribs ES_1 and FS_1 coming into the singular point S_1, and the line S_1bd where the two fold sheets b and d cross. The parabolic part of the swallowtail is so flattened as to be unrecognisable. Two sections of the swallowtail, l and m, are shown in the detail. The lines S_1a and S_1c which appear in the $t = -\epsilon$ section are omitted in the detail for clarity. The sequence of t sections of X shows how a generalised umbilic point can move from one region where $J > 0$ to another without crossing a $J = 0$ line.

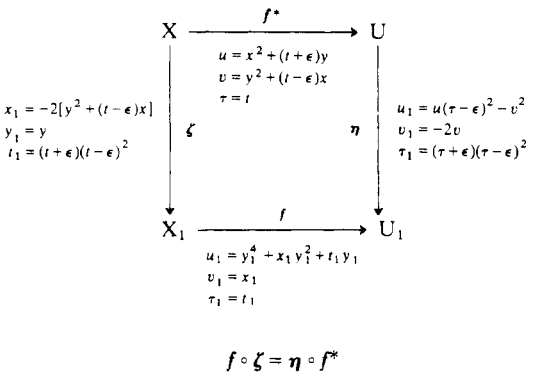

Figure 11. (*b*) These changes of coordinates ζ and η show that at $x = y = 0$ and $t = -\epsilon$ the singularity in the perturbed hyperbolic umbilic is actually a swallowtail. Note that the t_1 unfolding parameter multiplies the linear term in y_1 in the swallowtail $X_1 \xrightarrow{f} U_1$. This is equivalent to slicing the swallowtail surface 'from the side.' Similar changes of coordinates can be constructed at $t = +\epsilon$.

does not come from a perturbation of the underlying generating function, the hyperbolic umbilic point decomposes into two swallowtail points.

Similarly, the elliptic umbilic singularity can be destroyed by a small perturbation (figure 12). The elliptic umbilic $u = x^2 - y^2 + tx$, $v = -2xy + ty$ (obtained from the expression for ϕ in (4) after suitable scalings) has a vanishing Jacobian on a circle in X with radius equal to $\frac{1}{2}|t|$. The event occurs at $t = 0$ when the circle vanishes momentarily. By perturbing the equations, adding $-\epsilon y$ to u and ϵx to v, the radius of the $J = 0$ circle never vanishes; so there is no event.

Thus, two of the singularities on Thom's list which are stable with respect to perturbations of the generating function are not stable with respect to the larger class of perturbations to f itself. The remaining singularities—the fold, cusp and swallowtail—are the only singularities in maps $\boldsymbol{R}^3 \to \boldsymbol{R}^3$ which are stable with respect to

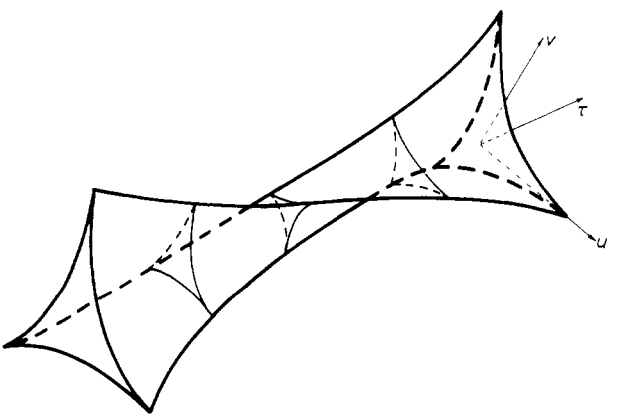

Figure 12. The singular set in (u, v, τ) for the perturbed elliptic umbilic given in the text has a twist of 120° near $\tau = 0$. The sense of the twist is determined by the sign of ϵ. The image of a generalised umbilic point runs down the centre of the figure.

arbitrary perturbations (see, for example, Golubitsky and Guillemin, 1973, p 191). Standard forms for these are given in table 4. To construct a time-dependent two-dimensional flow field from one of the forms in table 4 entails making transformations

$$(x_1, x_2, x_3) \leftrightarrow (x, y, t),$$

$$(u_1, u_2, u_3) \leftrightarrow (u, v, \tau)$$

in any smooth and non-singular way which produces $\tau = t$. The evolution of the two-dimensional flow field is obtained by taking simultaneous t and τ sections. Events occur when a τ section contains a swallowtail point or when a curved rib touches a τ section. As already mentioned, such a tangency can happen in two ways—beak-to-beak and lips.

Table 4. Stable singularities of functions $f: \boldsymbol{R}^3 \to \boldsymbol{R}^3$.

Singularity	Vector function f
Fold	$u_1 = x_1^2$ $u_2 = x_2$ $u_3 = x_3$
Cusp	$u_1 = x_1^3 + x_2 x_1$ $u_2 = x_2$ $u_3 = x_3$
Swallowtail	$u_1 = x_1^4 + x_3 x_1^2 + x_2 x_1$ $u_2 = x_2$ $u_3 = x_3$

The result is that, if perturbations are allowed in the vector field itself, the events are only three in number: beak-to-beak, lips and swallowtail. This contrasts with the case where perturbations are allowed only in the generating function, for then two additional events are possible: the hyperbolic and elliptic umbilics.

We have seen at the end of § 4, with the cusp as an example, that time-dependent two-dimensional flows can be derived from generating functions, and that this result is not restricted to irrotational and incompressible flows. In fact, local generating functions can be written down in a similar fashion for all the stable singularities and events under discussion. A generating function can also be written down for a regular point, namely $\Phi = \frac{1}{2}\boldsymbol{x}' \cdot \boldsymbol{x}' - \boldsymbol{u} \cdot \boldsymbol{x}'$, which gives $\boldsymbol{u} = \boldsymbol{x}' = \boldsymbol{f}(\boldsymbol{x})$, where $\boldsymbol{f}$ is non-singular. It follows that for any flow having stable singularities it is always possible to write down a local generating function. Since stability is a generic property (Mather 1971) the local behaviour of almost every flow can be described by a generating function. Knowing this it is irrelevent to ask whether a flow has a generating function. As we have emphasised, the important issue is what class of perturbations is suggested by the physics of the problem.

5.1. The velocity field of sea ice

The velocity field of sea ice already introduced in § 2.3 is an example of a flow field

subject to general perturbations. We now look at it in more detail. Velocity measurements made every three hours at about 25 points are used here. Standard least-squares techniques have been used to fit a fourth-order polynomial in x and y (15 coefficients) to each velocity component, at each time.

The sequence of t-sections shown in figure 13 was constructed from the polynomial fits at 06 00 GMT and 09 00 GMT on 3 May 1976. Because the (u, v) sections corresponding to those times were rather different in appearance, two intermediate figures were created by interpolating the polynomial coefficients to 07 00 and 08 00. In the sequence beak-to-beak events occur between the first and second and between

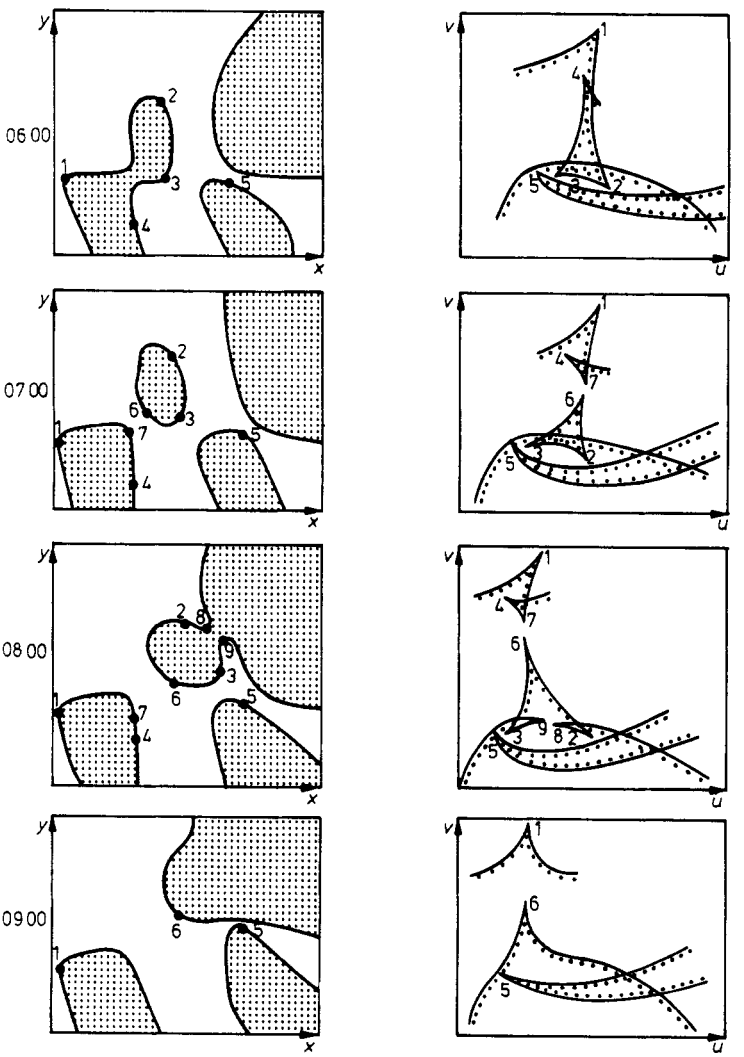

Figure 13. Singularities in the flow of sea ice. The singular set (fold-lines and cusp-points) is shown in X and its image in U for four times on 3 May 1976. Figure 4 is an expanded view of part of the first of these fields. Cusp-points and their images are indicated by number. Here the X-space measures 600 km square and U is roughly 10 cm s^{-1} square. J-positive regions in X-space are shaded.

the second and third sections. Three swallowtail events occur between the third and fourth sections. In contrast to the geostrophic flow example in figure 9, there are no restrictions on the merging together of J-positive regions. We note (as pointed out to us by Professor E C Zeeman) that the hyperbolic and elliptic umbilics, although unstable in a map of $\boldsymbol{R}^3 \to \boldsymbol{R}^3$, can be stable in a map of $\boldsymbol{R}^4 \to \boldsymbol{R}^4$ (Golubitsky and Guillemin 1973, p 191). This may account for the patterns in figure 13 that look close to umbilic singularities. The higher-dimensional singularity is acting as an 'organising centre'.

As with the field of the geostrophic wind, we are impressed by the richness of the images: all the sections we have examined have contained folds and cusps; events are common and, in the sequence given here, several events occur during a single three-hour time interval.

5.2. Classification of generalised umbilic and antiumbilic points

The classification of umbilic points given by Berry and Hannay (see § 4.2) applies when the function $\boldsymbol{f}: \boldsymbol{R}^2 \to \boldsymbol{R}^2$ is derived from a surface, the umbilic points being defined and classified in terms of its curvatures. But in the general case $\boldsymbol{f}$ is not derived from a surface. Nevertheless, a classification (appendix 3) of generalised umbilic points, analogous to the Berry–Hannay scheme, can be constructed by using the $\boldsymbol{a}$ and $\boldsymbol{a}_\perp$ directions associated with L in place of the curvature directions ($\boldsymbol{a}$ and $\boldsymbol{a}_\perp$ *are* the curvature directions when a surface exists). The classification uses the same three qualities, index ($\pm\frac{1}{2}$), number of straight lines (3 or 1) and contour (elliptic or hyperbolic); (the word *contour* is used in place of *catastrophe* because there is now no catastrophe associated with elliptic or hyperbolic umbilic points). Of the classes defined by the eight combinations only two are now empty: those involving negative index and one line simultaneously. There are thus two new possiblities +3E and +1E in the absence of a surface.

The classification in this form applies (appendix 3) without change to generalised antiumbilic points also.

To give examples, there are two generalised umbilic points in figure 4(*b*) and three generalised antiumbilic points. Using u for umbilic and ū for antiumbilic they classify as follows:

Point	Code
1	u−3H
2	u+1H
3	ū−3H
4	ū+1H
5	ū−3H.

Points 4 and 5 did not exist in an earlier image. We can infer that the two antiumbilic points formed as ū−3H and ū+3H and then point 4 had the transition ū+3H→ ū+1H.

Although the points can be classified by evaluating the discriminants given in appendix 3, we have instead relied on diagrams similar to that in figure 4(*b*). For some points, considerable enlargement of the diagrams is required to identify the pattern. For point 2, for instance, a magnification of 100× was needed to determine that the

line classification was 1 rather than 3. To determine the contour classification, we have used contour plots of the eigenvalues of $\mathbf{L}^T\mathbf{L}$. Elliptic points are distinguished by local extremes of the eigenvalues λ_1, and λ_2, where $\lambda_1 \geqslant \lambda_2$. It is notable that all the points in this image, the only points we have classified, are hyperbolic. For a Gaussian random surface with isotropic disorder Berry and Hannay calculate that hyperbolic umbilic points are statistically 2·73 times more frequent than elliptic umbilic points. Often a pair of generalised umbilic and antiumbilic points are seen near to a fold-line, as are points 2 and 5. We have not reconciled this observation with our conclusion in appendix 3 that generalised umbilic and antiumbilic points cannot interact.

The classification of appendix 3 also applies to the 'isotropic points' in any two-dimensional field of a symmetric tensor, a stress field for example. If the direction of greater (or lesser) principal stress is identified with the $\boldsymbol{a}$ direction, the points where the stress is isotropic correspond to generalised umbilic points. We say *generalised* umbilic points rather than umbilic points because there will be, in general, no surface for which the stress trajectories (lines parallel to directions of principal stress) are the lines of curvature. Often (for example, where an Airy-type stress function exists) such a surface may be constructed and the isotropic points are then the umbilic points of this surface, but this is not the general case. The same applies to a distribution of elastic strain even when there is no unique displacement function ('incompatible' strain)—for none of the analysis in appendix 3 for the classification of generalised umbilic points assumes that the symmetric tensor under discussion (stress, strain or $\mathbf{L}^T\mathbf{L}$) is the gradient of a vector. So the positive and negative isotropic points of photoelasticity (Jessop and Harris 1949)†, for example, are generalised umbilic points, and there are six different kinds.

6. Discussion

The physical scientist might reasonably ask whether the introduction of the concepts and vocabulary of singularity theory contributes to his understanding of flow fields. After all, are there not already so many kinematic descriptions in use that it is difficult to keep them clear in one's mind? Our reply is to point to the simplicity of the results—in the general case (§ 5) there are only three possible singular events—and to the strong geometric and topological character of the singularities. Many apparently complex situations can be analysed completely using only a geometric understanding of the basic singularities, and no computation.

That these singularities persist under arbitrary coordinate changes makes them more fundamental than the familiar invariants, such as the divergence, which are stable only with respect to coordinate changes which preserve the metric. In the case of geophysical flow fields, for example, one can note that different investigators of the same field might choose different geographical map projections, and if one chose a Mercator projection he would find that the divergence was not immediately clear; but the number and type of singularities would be the same for all map projections.

The kinematic description of time-dependent two-dimensional flow fields given here applies without modification to other physical situations; it becomes a question of naming the variables. Electric or magnetic field distributions are an obvious example.

† For good examples of positive and negative isotropic points, see figure 154, p. 161, which illustrates a railway coupling hook—one of the few generic shapes to be found in any book on photoelasticity.

If $\boldsymbol{E}$ or $\boldsymbol{H}$ derives from an underlying time-dependent scalar potential the events in those fields, as they evolve with time, will be the longer list of five. But if, as is the general case, there is no such underlying potential, we can conclude that the shorter list of three will apply.

We should emphasise that, although we have not discussed the problem of singularities in time-dependent three-dimensional fields, our analysis does apply to three-dimensional situations. Take the wind as an example. The horizontal *component* of the wind at any given level in the atmosphere is a changing two-dimensional vector field whose singular events are classified by this paper. There may be higher-order singularities which occur at special places in the atmosphere at special times—we have not studied these (they could presumably be analysed by extending the method used in § 5)—but such higher-order events will be missed by an arbitrarily chosen horizontal slice of the atmosphere.

Our analysis applies also to singularities in a mapping of a three-dimensional vector field at a given time. Take the example of an electric field. If $\boldsymbol{E} = -\text{grad}\,\phi$, we map from (x, y, z) into the space of the components (E_1, E_2, E_3) and note that $\boldsymbol{E}$ results from the condition that the generating function

$$\Phi = \phi + E_1 x + E_2 y + E_3 z$$

should be stationary. It follows that the singularities in $\boldsymbol{E}$-space observed generically will be the five in Thom's list for which the dimension of the control space is $\leqslant 3$: the fold, cusp, swallowtail, elliptic umbilic and hyperbolic umbilic. If div $\boldsymbol{E} = \rho$, where ρ is the charge density, there is a constraint $\nabla^2\phi = -\rho$ on the distribution of ϕ, analogous to the surface tension condition in the water-drop example of § 4.3, and there will be some corresponding constraint on the catastrophe surfaces in $\boldsymbol{E}$-space.

On the other hand, if $\boldsymbol{E}$ is not derivable from a scalar potential (because of electromagnetic induction), it becomes a matter of the degrees of freedom allowed by the physical situation. If the field distribution can be quite general, only the fold, cusp and swallowtail will be seen.

One of the purposes of this work was to find an answer to the question 'what constitutes qualitative agreement between two flow fields?' A predicted flow field will not agree exactly with a measured one, but when shall we say the two are similar? We suggest that two vector fields are fundamentally dissimilar if they differ in the number and type of their singularities (the two fields being examined with the same level of detail). To give the simplest example, the introduction of a new fold changes drastically the number of points in the flow field having a given velocity.

Finally, we mention an application of the present work in the design of experiments. Most experimental apparatus is designed to produce a physical condition of high symmetry, because it is easier to analyse. But, if one tries to produce a vector field, perhaps a magnetic field, having an unstable (non-generic) singularity, one knows that imperfections of materials and workmanship must inevitably preclude complete success. On the other hand, little skill is needed to produce a generic singularity, even though it may not be in just the intended place. Therefore, to know which singularities are generic and which are not is a useful aid to efficient and economical design.

In a wider context, to distinguish those things that are stable from those that are not is basic to an understanding of why nature prefers the structures and events that it does.

Acknowledgments

We thank Dr T Poston for commenting on an early draft of this paper and M Albright for providing the atmospheric pressure fields. We also thank Dr D Rand and Dr J P Cleave for advice and criticism. The work was supported in large part by the National Science Foundation Grant 0PP71-09031 to the University of Washington for the Arctic Sea Ice Study.

Appendix 1. Relation to the work of Berry and Mackley

A related application of catastrophe theory to a problem of fluid flow is the work of Berry and Mackley (1977) on the 'six-roll mill'. They apply catastrophe theory differently from the way described here and it is useful to clarify the relation between the two points of view.

Berry and Mackley study a special two-dimensional, steady, incompressible, flow field (figure 14) which is controlled by the speeds of six rollers. At the origin in X the velocity is zero. Three streamlines enter the origin and three emerge from it. This flow is unstable in the sense that a generic perturbation, caused by changing the speeds of the rollers, makes the point of zero velocity at the origin break up into several separated points of zero velocity, with an accompanying change in the topology of the streamlines. From the point of view of Berry and Mackley the changes in the number of points in X with zero velocity, and the resulting changes in the topology of the streamlines, are the catastrophes.

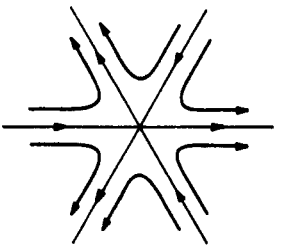

Figure 14. The streamline pattern in X-space for the unstable flow field associated with the elliptic umbilic catastrophe and studied by Berry and Mackley (1977).

Their analysis proceeds as follows. The stream function of the singular unperturbed flow is $\frac{1}{3}x^3 - xy^2$. If one adds to this a uniform translational flow with velocity $\boldsymbol{V} = (V_x, V_y)$ and a uniform rotation rate ω_0, the stream function becomes

$$\psi = \tfrac{1}{3}x^3 - xy^2 - \tfrac{1}{2}\omega_0(x^2 + y^2) - V_y x + V_x y.$$

This is the universal unfolding of the unperturbed flow. Now ψ has the form of the generating function for the elliptic umbilic catastrophe, with (x, y) as state variables, and (ω_0, V_x, V_y) as control variables. To each choice of (ω_0, V_x, V_y) there corresponds a particular field of flow. As these control parameters are changed the flow field changes. If ψ is regarded as a generating function (this is the crucial difference from the scheme of this paper where the generating function would be $\psi - uy + vx$), the

condition that the gradient vanishes is that

$$\frac{\partial\psi}{\partial x} = -v = 0 \qquad \text{and} \qquad \frac{\partial\psi}{\partial y} = u = 0;$$

in other words, the gradient condition picks out the points in state space where the velocity is zero. When the point (ω_0, V_x, V_y) in control space crosses the elliptic umbilic catastrophe surface (figure 6(*c*)) the number of zeros in the flow field changes by two, this being accomplished by the creation or annihilation of a pair, exactly as in figure 5(*a*). If the point in control space passes from the inside to the outside of the catastrophe surface through a rib, three zeros in the flow field come together and turn into one (as in figure 5(*b*)). The catastrophes are these changes in the number of zeros, and in the topology of the streamlines, as the control variables are changed.

From the point of view of the present paper, if we map the flow field described by ψ, with general values of ω_0, V_x, V_y, into the (u, v) plane we obtain the folds and cusps shown in figure 15. The generating function is now

$$\Phi = \psi - uy + vx = \tfrac{1}{3}x^3 - xy^2 - \tfrac{1}{2}\omega_0(x^2 + y^2) - (V_y - v)x + (V_x - u)y$$

and the gradient condition is

$$\frac{\partial\Phi}{\partial x} = \frac{\partial\psi}{\partial x} + v = 0 \qquad \text{and} \qquad \frac{\partial\Phi}{\partial y} = \frac{\partial\psi}{\partial y} - u = 0.$$

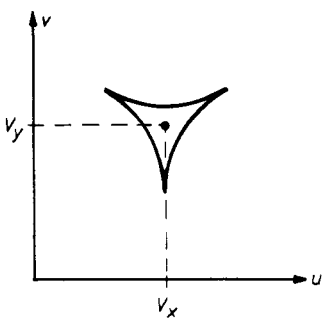

Figure 15. The folds and cusps in the (u, v) plane for the general flow studied by Berry and Mackley (1977).

This condition describes the whole velocity field in (x, y) space (not simply the points of zero velocity). Catastrophes in the form of folds and cusps already exist, from this point of view, even with general values of the parameters ω_0, V_x and V_y. Their meaning is that as the control point (u, v) moves across a fold, for example, the number of points in the flow field with that velocity changes by two. The fold and cusp catastrophes are properties of *this* particular flow field; they are not a consequence of a *change* in the flow field.

Suppose V_x and V_y are now changed, ω_0 being kept fixed. Physically, this means that the same translational velocity is added at every point of the field, and so the diagram in velocity space with its cusps and folds is simply translated rigidly. If this translation makes a fold sweep through the origin, the number of points in the field with zero velocity will change by two. This event is a fold catastrophe in the sense of

Berry and Mackley. A similar argument applies when a cusp sweeps through the origin. We see that even with the same family of flow fields it is possible to label as 'catastrophes' forms and events which are physically quite different.

Appendix 2. Procedure for inspecting singularities

Given polynomial representations for $u(x, y)$ and $v(x, y)$, these steps were used to sketch the folds and cusps for each t-section:

(1) For a rectangular region in X define a grid of points (x_i, y_j); $i, j = 1, \ldots, N$.

(2) At each grid point evaluate the Jacobian, J_{ij}.

(3) Check along each side of each cell to see if J changes sign. If so, interpolate to find coordinates (x_k, y_k) such that $J(x_k, y_k) = 0$. This will happen 0, 2 or 4 times for each cell. Evaluate $u_k = u(x_k, y_k)$ and $v_k = v(x_k, y_k)$. Store x_k, y_k, u_k, v_k; $k = 1, \ldots, K$.

(4) Plot these points in X and U, joining the pairs 1–2, 3–4, ..., by straight lines. This draws the fold-lines in X and their images in U. The correspondence between lines in X and lines in U can be established from a print-out of the points (x_k, y_k) and (u_k, v_k), $k = 1, \ldots, K$.

(5) To locate cusp-points in X, determine the direction $\boldsymbol{a}$ at each grid point using $\boldsymbol{a} = (\cos\theta, \sin\theta)$, where

$$\tan 2\theta = \frac{2(u_x u_y + v_x v_y)}{u_x^2 - u_y^2 + v_x^2 - v_y^2}$$

and θ or $\theta + \frac{1}{2}\pi$ is chosen depending on which minimises $|\mathbf{L}\boldsymbol{n}|$. A unit vector in the $\boldsymbol{a}$ direction is plotted at each grid point in X. In this display, cusp-points are points where $\boldsymbol{a}$ is tangent to a fold-line.

(6) Umbilic points and their generalisation can be found by plotting zero contours of $u_x - v_y$ and $u_y + v_x$ and finding their intersections, and antiumbilic points and their generalisations by plotting zero contours of $u_x + v_y$ and $u_y - v_x$. These points can also be located by inspecting the field of $\boldsymbol{a}$ vectors, to find points where $\boldsymbol{a}$ is indeterminate.

(7) A short-cut procedure is to plot u and v contours in X. Fold points are points of tangency between a u and a v contour. The direction $\boldsymbol{a}$ is in the mutually tangent direction. A fold-line can quickly be sketched and the cusp-points identified. One advantage of this plot is that it is relatively easy to count the number of inverse images of a point (u, v). Another is that umbilic points are points where the two sets of contours intersect to form squares.

Appendix 3. Classification of generalised umbilic and antiumbilic points

First consider a generalised umbilic point. The directions $\boldsymbol{a}$ and $\boldsymbol{a}_\perp$ are the eigenvectors of $\mathbf{L}^T\mathbf{L}$. After adjusting coordinates so that the umbilic point is at the origin, the linear approximation to $\mathbf{L}^T\mathbf{L}$ can be written

$$\begin{pmatrix} K + \alpha x + \beta y & \beta_1 x + \gamma_1 y \\ \beta_1 x + \gamma_1 y & K + \gamma x + \delta y \end{pmatrix}.$$

This uses no special properties of $\mathbf{L}^T\mathbf{L}$ and so the classification which follows applies to any symmetric tensor at an umbilic point.

The *index* of an umbilic point, as defined in § 4.2, is $\pm\frac{1}{2}$ according to the sign of the discriminant D_I:

$$D_I = (\alpha - \gamma)\gamma_1 + (\delta - \beta)\beta_1.$$

The *line* classification is 1 or 3 depending on the number of straight $\boldsymbol{a}$ trajectories emerging from an umbilic point. Suppose the point (x, y) lies on a straight $\boldsymbol{a}$ trajectory emerging from the origin. Then (x, y) must be an eigenvector of $\mathbf{L}^T\mathbf{L}$ at (x, y). This leads to a cubic which has one or three roots depending on the discriminant D_L:

$$D_L = 4[3\gamma_1(\alpha - \gamma - \gamma_1) - (\delta - \beta - \beta_1)^2][3\beta_1(\delta - \beta - \beta_1) - (\alpha - \gamma - \gamma_1)^2]$$
$$-[(\delta - \beta - \beta_1)(\alpha - \gamma - \gamma_1) - 9\beta_1\gamma_1]^2.$$

If D_L is positive, there are three lines; if D_L is negative, there is one line.

Finally, umbilic points can be classified as elliptic or hyperbolic according to whether the *contours* of constant eigenvalue of $\mathbf{L}^T\mathbf{L}$ are elliptic or hyperbolic. (This is not related to catastrophes in the generalised case.) Equivalently, the sign of the Gaussian curvature of the surface given by the determinant of $\mathbf{L}^T\mathbf{L}$ can be used. The appropriate discriminant is

$$D_C = 4(\alpha\gamma - \beta_1^2)(\beta\delta - \gamma_1^2) - (\alpha\delta + \beta\gamma - 2\beta_1\gamma_1)^2.$$

The point is elliptic if the discriminant is positive and hyperbolic if it is negative.

The classification applies without alteration to antiumbilic points; for, even if $\mathbf{L}$ has an antiumbilic form at $\boldsymbol{x}$, $\mathbf{L}^T\mathbf{L}$ has an umbilic form. Thus the complete classification is (J, D_I, D_L, D_C) where

	J	D_I	D_L	D_C
>0	umbilic	index $+\frac{1}{2}$	3 lines	elliptic
<0	antiumbilic	index $-\frac{1}{2}$	1 line	hyperbolic

Of the sixteen categories, those involving negative index and one line simultaneously are empty since these conditions are incompatible. This leaves 12 possible categories—6 for generalised umbilics and 6 for generalised antiumbilics.

As the flow field varies (with time, say) the entries in $\mathbf{L}^T\mathbf{L}$ will vary continuously and so will J, D_I, D_L, and D_C. A generalised umbilic point will move from one category to another when one of the discriminants passes through zero. But the discriminants do not vary independently and so only certain transitions are possible. They are governed by the following rules:

(1) A generalised umbilic or antiumbilic point can never lie on a $J = 0$ line. To do so would require the hyperbolic or elliptic umbilic catastrophe, which, as noted in § 5, cannot happen stably for general fields. Thus, generalised umbilic and antiumbilic points remain on opposite sides of fold-lines and do not interact. A generalised umbilic point cannot evolve into a generalised antiumbilic point.

(2) It follows from the circuit definition of index (§ 4.2) that only points of opposite index can be born in pairs or annihilate each other.

(3) When two generalised umbilic or antiumbilic points are born or annihilate generically, they will have the same J and D_C classification, and D_L must be positive.

(4) For umbilic points (see table 3) there are no elliptic points with index $+\frac{1}{2}$. Therefore, elliptic umbilic points cannot be born as twins or mutually annihilate one

another. In the non-generalised case only pairs of hyperbolic points are born or annihilate one another. In the general case, however, there are elliptic points of positive index and so this argument does not apply. Elliptic umbilic points can transform into hyperbolic points without otherwise altering their classification.

(5) A generalised umbilic point having $D_L > 0$ (three lines) can transform continuously into one with $D_L < 0$ (one line) and this is the only way $D_L < 0$ points are made.

References

Albright M 1977 *Symposium on Sea Ice Processes and Models, Seattle, Washington, September 6–9, 1977* Preprints, vol. 1, 133–41

Benjamin T B 1978 *Proc. R. Soc.* A **359** 1–43

Berry M V 1976 *Adv. Phys.* **25** 1–26

Berry M V and Hannay J H 1977 *J. Phys. A: Math. Gen.* **10** 1809–21

Berry M V and Mackley M R 1977 *Phil. Trans. R. Soc.* A **287** 1–16

Berry M V and Nye J F 1977 *Nature* **267** 34–36

Golubitsky M and Guillemin V 1973 *Stable Mappings and Their Singularities* (New York: Springer)

Jessop H T and Harris F C 1949 *Photoelasticity: Principles and Methods* (London: Cleaver-Hume) pp 74–7

Lacher R C, McArthur R and Buzyna G 1977 *Am. Scientist* **65** 614–21

Mather J N 1971 *Proceedings of Liverpool Singularities Symposium I: Lecture Notes in Mathematics No. 192* (New York: Springer) pp 207–53

Nye J F 1978 *Proc. R. Soc.* A **359** 21–41

Poston T and Stewart I N 1976 *Research Notes in Mathematics* vol. 7 (London: Pitman)

Thom R 1975 *Structural Stability and Morphogenesis* (Reading, Mass: Benjamin) (Translation of *Stabilité Structurelle et Morphogénèse* 1972 (Reading, Mass: Benjamin))

Wassermann G 1975 *Acta Math.* **135** 57–128

Whitney H 1955 *Ann. Math., NY* **62** 374–410